87. Race, R.E., Priola, S.A., Bessen, R.A., Ernst, D., Dockter, J., Rall, G.F., Mucke, L., Chesebro, B. and Oldstone, M.B. 1995. *Neuron* **15**: 1183–1191.
88. Raeber, A.J., Race, R.E., Brandner, S., Priola, S.A., Sailer, A., Bessen, R.A., Mucke, L., Manson, J., Aguzzi, A., Oldstone, M.B., Weissmann, C. and Chesebro, B. 1997. *EMBO J.* **16**: 6057–6065.
89. Ramasamy, I., Law, M., Collins, S. and Brooke, F. 2003. *Lancet Infect. Dis.* **3**: 214–222.
90. Raymond, G.J., Hope, J., Kocisko, D.A., Priola, S.A., Raymond, L.D., Bossers, A., Ironside, J., Will, R.G., Chen, S.G., Petersen, R.B., Gambetti, P., Rubenstein, R., Smits, M.A., Lansbury, P.T. Jr. and Caughey, B.1997. *Nature* **388**: 285–288.
91. Rhie, A., Kirby, L., Sayer, N., Wellesley, R., Disterer, P., Sylvester, I., Gill, A., Hope, J., James, W. and Tahiri-Alaoui, A. 2003. *J. Biol. Chem.* **278**: 39697–39705.
92. Ritchie, D.L., Head, M.W. and Ironside, J.W. 2004. *Neuropathol. Appl. Neurobiol.* **30**: 360–368.
93. Rogers, M., Yehiely, F., Scott, M. and Prusiner, S.B. 1993. *Proc. Natl. Acad. Sci. U.S.A.* **90**: 3182–3186.
94. Rubenstein, R., Carp, R.I. and Callahan, S.M. 1984. *J. Gen. Virol.* **65**: 2191–2198.
95. Saá, P., Castilla, J. and Soto, C. 2006. *Science* **313**: 92–94.
96. Saborio, G.P., Permanne, B. and Soto, C. 2001. *Nature* **411**: 810–813.
97. Safar, J., Wille, H., Itri, V., Groth, D., Serban, H., Torchia, M., Cohen, F.E. and Prusiner, S.B. 1998. *Nat. Med.* **4**: 1157–1165.
98. Sakudo, A., Suganuma, Y., Kobayashi, T., Onodera, T. and Ikuta, K. 2006. *Biochem. Biophys. Res. Commun.* **341**: 279–284.
99. Sakudo, A., Lee, D.C., Saeki, K., Matsumoto, Y., Itohara, S. and Onodera, T. 2003. *Biochem. Biophys. Res. Commun.* **310**: 725–729.
100. Sakudo, A., Onodera, T., Suganuma, Y., Kobayashi, T., Saeki, K. and Ikuta, K. 2006. *Mini. Rev. Med. Chem.* **6**: 589–601.
101. Sakudo, A., Tsenkova, R., Onozuka, T., Morita, K., Li, S., Warachit, J., Iwabu, Y., Li, G., Onodera, T. and Ikuta, K. 2005. *Microbiol. Immunol.* **49**: 695–701.
102. Sakudo, A., Lee, D.C., Li, S., Nakamura, T., Matsumoto, Y., Saeki, K., Itohara, S., Ikuta, K. and Onodera, T. 2005. *Biochem. Biophys. Res. Commun.* **328**: 14–19.
103. Sakudo, A., Lee, D.C., Nakamura, I., Taniuchi, Y., Saeki, K., Matsumoto, Y., Itohara, S., Ikuta, K. and Onodera, T. 2005. *Biochem. Biophys. Res. Commun.* **333**: 448–454.
104. Sakudo, A., Lee, D.C., Nishimura, T., Li, S., Tsuji, S., Nakamura, T., Matsumoto, Y., Saeki, K., Itohara, S., Ikuta, K. and Onodera, T. 2005. *Biochem. Biophys. Res. Commun.* **326**: 600–606.
105. Sakudo, A., Lee, D.C., Saeki, K., Nakamura, Y., Inoue, K., Matsumoto, Y., Itohara, S. and Onodera, T. 2003. *Biochem. Biophys. Res. Commun.* **308**: 660–667.
106. Sakudo, A., Lee, D.C., Yoshimura, E., Nagasaka, S., Nitta, K., Saeki, K., Matsumoto, Y., Lehmann, S., Itohara, S., Sakaguchi, S. and Onodera, T. 2004. *Biochem. Biophys. Res. Commun.* **313**: 850–855.
107. Sayer, N.M., Cubin, M., Rhie, A., Bullock, M., Tahiri-Alaoui, A. and James, W. 2004. *J. Biol. Chem.* **279**: 13102–13109.
108. Schätzl, H.M., Laszlo, L., Holtzman, D.M., Tatzelt, J., DeArmond, S.J., Weiner, R.I., Mobley, W.C. and Prusiner, S.B. 1997. *J. Virol.* **71**: 8821–8831.
109. Schmerr, M.J., Jenny, A.L., Bulgin, M.S., Miller, J.M., Hamir, A.N., Cutlip, R.C. and Goodwin, K.R. 1999. *J. Chromatogr. A* **853**: 207–214.
110. Schmitt, J., Beekes, M., Brauer, A., Udelhoven, T., Lasch, P. and Naumann, D. 2002. *Anal. Chem.* **74**: 3865–3868.
111. Schoch, G., Seeger, H., Bogousslavsky, J., Tolnay, M., Janzer, R.C., Aguzzi, A. and Glatzel, M. 2006. *Plos Med.* **3**: e14.
112. Schreuder, B.E. and Somerville, R.A. 2003. *Rev. Sci. Tech.* **22**: 103–120.
113. Schreuder, B.E., van Keulen, L.J., Vromans, M.E., Langeveld, J.P. and Smits, M.A. 1996. *Nature* **381**: 563.
114. Schulz-Schaeffer, W.J., Tschöke, S., Kranefuss, N., Dröse, W., Hause-Reitner, D., Giese, A., Groschup, M.H. and Kretzschmar, H.A. 2000. *Am. J. Pathol.* **156**: 51–56.
115. Scott, M., Foster, D., Mirenda, C., Serban, D., Coufal, F., Wälchli, M., Torchia, M., Groth, D., Carlson, G. and DeArmond, S.J. 1989. *Cell* **59**: 847–857.
116. Scott, M., Groth, D., Foster, D., Torchia, M., Yang, S.L., DeArmond, S.J. and Prusiner, S.B. 1993. *Cell 73*: 979–988.
117. Seeger, H., Heikenwalder, M., Zeller, N., Kranich, J., Schwarz, P., Gaspert, A., Seifert, B., Miele, G. and Aguzzi, A. 2005. *Science* **310**: 324–326.
118. Serban, A., Legname, G., Hansen, K., Kovaleva, N. and Prusiner, S.B. 2004. *J. Biol. Chem.* **279**: 48817–48820.
119. Shaked, G.M., Shaked, Y., Kariv-Inbal, Z., Halimi, M., Avraham, I. and Gabizon, R. 2001. *J. Biol. Chem.* **276**: 31479–31482.
120. Shmerling, D., Hegyi, I., Fischer, M., Blättler, T., Brandner, S., Götz, J., Rülicke, T., Flechsig, E., Cozzio, A., von Mering, C., Hangartner, C., Aguzzi, A. and Weissmann, C. 1998. *Cell* **93**: 203–214.
121. Solassol, J., Crozet, C. and Lehmann, S. 2003. Prion propagation in cultured cells. *Br. Med. Bull.* **66**: 87–97.
122. Soto, C., Saborio, G.P. and Anderes, L. 2002. *Trends Neurosci.* **25**: 390–394.
123. Tanji, K., Saeki, K., Matsumoto, Y., Takeda, M., Hirasawa, K., Doi, K., Matsumoto, Y. and Onodera, T. 1995. *Intervirology* **38**: 309–315.
124. Taraboulos, A., Jendroska, K., Serban, D., Yang, S.L., DeArmond, S.J. and Prusiner, S.B. 1992. *Proc. Natl. Acad. Sci. U.S.A.* **89**: 7620–7624.
125. Telling, G.C., Haga, T., Torchia, M., Tremblay, P., DeArmond, S.J. and Prusiner, S.B. 1996. *Genes Dev.* **10**: 1736–1750.
126. Telling, G.C., Scott, M., Hsiao, K.K., Foster, D., Yang, S.L., Torchia, M., Sidle, K.C., Collinge, J., DeArmond, S.J. and Prusiner, S.B. 1994. *Proc. Natl. Acad. Sci. U.S.A.* **91**: 9936–9940.
127. Thomzig, A., Kratzel, C., Lenz, G., Krüger, D. and Beekes, M. 2003. *EMBO Rep.* **4**: 530–533.
128. Thomzig, A., Schulz-Schaeffer, W., Kratzel, C., Mai, J. and Beekes, M. 2004. *J. Clin. Invest.* **113**: 1465–1472.
129. Thuring, C.M., Erkens, J.H., Jacobs, J.G., Bossers, A., Van Keulen, L.J., Garssen, G.J., Van Zijderveld, F.G., Ryder, S.J., Groschup, M.H., Sweeney, T. and Langeveld, J.P. 2004. *J. Clin. Microbiol.* **42**: 972–980.
130. van Keulen, L.J., Schreuder, B.E., Vromans, M.E., Langeveld, J.P. and Smits, M.A. 2000. *Arch. Virol. (Suppl.)* **16**: 57–71.
131. Vilette, D., Andreoletti, O., Archer, F., Madelaine, M.F., Vilotte, J.L., Lehmann, S. and Laude, H. 2001. *Proc. Natl. Acad. Sci. U.S.A.* **98**: 4055–4059.
132. Vorberg, I., Chan, K. and Priola, S.A. 2001. *J. Virol.* **75**: 10024–10032.
133. Vorberg, I., Raines, A. and Priola, S.A. 2004. *J. Biol. Chem.* **279**: 29218–29225.
134. Vorberg, I., Groschup, M.H., Pfaff, E. and Priola, S.A. 2003. *J. Virol.* **77**: 2003–2009.

135. Vorberg, I., Raines, A., Story, B. and Priola, S.A. 2004. *J. Infect. Dis.* **189**: 431–439.
136. Wadsworth, J.D., Hill, A.F., Beck, J.A. and Collinge, J. 2003. *Br. Med. Bull.* **66**: 241–254.
137. Wadsworth, J.D., Joiner, S., Hill, A.F., Campbell, T.A., Desbruslais, M., Luthert, P.J. and Collinge, J. 2001. *Lancet* **358**: 171–180.
138. Weiss, S., Proske, D., Neumann, M., Groschup, M.H., Kretzschmar, H.A., Famulok, M. and Winnacker, E.L. 1997. *J. Virol.* **71**: 8790–8797.
139. Westaway, D., Zuliani, V., Cooper, C.M., Da Costa, M., Neuman, S., Jenny, A.L., Detwiler, L. and Prusiner, S.B. 1994. *Genes Dev.* **8**: 959–969.
140. Wild, M.A., Spraker, T.R., Sigurdson, C.J., O'Rourke, K.I. and Miller, M.W. 2002. *J. Gen. Virol.* **83**: 2629–2634.
141. Winklhofer, K.F., Hartl, F.U. and Tatzelt, J. 2001. *FEBS Lett* **503**: 41–45.
142. Zanusso, G., Ferrari, S., Cardone, F., Zampieri, P., Gelati, M., Fiorini, M., Farinazzo, A., Gardiman, M., Cavallaro, T., Bentivoglio, M., Righetti, P.G., Pocchiari, M., Rizzuto, N. and Monaco, S. 2003. *New Engl. J. Med.* **348**: 711–719.
143. Zerr, I., Bodemer, M., Otto, M., Poser, S., Windl, O., Kretzschmar, H.A., Gefeller, O. and Weber, T. 1996. *Lancet* **348**: 846–849.

Visible and near-infrared (Vis-NIR) spectroscopy: Introduction and Perspectives for Diagnosis of Chronic Fatigue Syndrome

By Akikazu Sakudo[1]* Yukiko Hakariya[1], Takanori Kobayashi[1], and Kazuyoshi Ikuta[1]

[1]Department of Virology, Center for Infectious Disease Control, Research Institute for Microbial Diseases, Osaka University, Yamadaoka, Suita, Osaka 565-0871, Japan

To whom correspondence should be addressed:

Akikazu Sakudo, Department of Virology, Research Institute for Microbial Diseases, Osaka University, Yamadaoka, Suita, Osaka 565-0871, Japan

Tel.: ++81-6-6879-8307 Fax: ++81-6-6879-8310

E-mail: sakudo@biken.osaka-u.ac.jp

Summary

Currently, chronic fatigue syndrome (CFS) is diagnosed based on clinical symptoms. Although various information on psychological, endocrinological, and immunological abnormalities in CFS patients has been reported, there is no clear consensus, possibly due to the absence of an objective diagnostic method. One experimental approach is the use of instrumentation for diagnosis. Recently, our research group has shown the potential of visible and near-infrared (Vis-NIR) spectroscopy for the diagnosis of CFS using serum samples. This review will introduce the method and the future perspectives made possible by it.

Keywords:

Chronic fatigue syndrome; myalgia encephalomyelitis; visible and near-infrared spectroscopy; diagnosis

Introduction

Chronic fatigue syndrome (CFS) is a debilitating disorder involving persistent fatigue lasting for more than six months [1]. However, the difference between CFS and CFS-like diseases such as myalgia encephalomyelitis (ME), postviral fatigue syndrome (PVFS), chronic fatigue/immune dysfunction syndrome (CFIDS), and 'Yuppie flu' remains unclear. The symptoms of CFS include fatigue, pain, breathing problems, depression leading to digestive disturbances, low grade fever, difficulty in concentrating, and weakness of the immune system and muscles [1]. The symptoms are not resolved by sufficient rest [1].

The incidence of CFS is 0.4% in the United States and other countries [2] and 0.26% in Japan [3]. Economic losses caused by the disease are estimated at as high as 9.1 billion dollars per year in the United States [4] and 408 billion yen per year in Japan [3]. However, research conducted by the Centers for Disease Control and Prevention (CDC) estimates that less than 20% of CFS patients in the United States have been successfully diagnosed [2, 5], indicating that the number of patients will increase if more reliable diagnostic methods are established. The main barriers to identifying CFS patients are an absence of biophysical and biochemical signs that identify the disease and lack of diagnostic laboratory tests [6]. This may be at least in part due to the heterogeneity of the symptoms of CFS patients [6]. At present, CFS diagnosed based on the presentation of symptoms and exclusion of other medical entities.

Therefore, it relies on symptometology. Most published studies have diagnosed CFS on the basis of CDC criteria [1]. As psychiatric diseases and other treatable conditions are sometimes difficult to distinguish from CFS, the patient's

Fig. 1. *Our research group*

Medical spectroscopy group at Department of Virology, Research Institute for Microbial Diseases, Osaka University was composed of a virologist (Kazuyoshi Ikuta), spectroscopist (Akikazu Sakudo), physician (Yukiko Hakariya), and clinical laboratory technologist (Takanori Kobayashi). Researchers with different backgrounds are studying CFS.

*(continued **on** page 9)*

Visible and near-infrared (Vis-NIR) spectroscopy: Introduction and Perspectives for Diagnosis of CFS

symptoms should carefully be examined. Physicians should, through a careful investigation of the patient's medical history and appropriate testing, rule out other diseases including mononucleosis, Lyme disease, thyroid conditions, diabetes, multiple sclerosis, various cancers, depression and bipolar disorder.

We feel that the main problems in CFS studies can be attributed to the objectivity of diagnosis and absence of biomarkers. Our research group, composed of a virologist, spectroscopist, physician, and clinical laboratory technologist, has been studying visible and near-infrared (Vis-NIR) spectroscopy (Fig. 1). We decided to apply Vis-NIR spectroscopy to the study of CFS. In this review, we introduce the method and its possible uses for CFS research.

Vis-NIR spectroscopy and multivariate analysis

The short wavelength (SW)-NIR region and the red region, the so called "optical window" from 600 to 1,100 nm, are together the most useful region for measuring biological samples [7].

The absorption of hemoglobin and water is extensive in the region below 600 nm and above 1,100 nm, respectively, which limits spectroscopic and microscopic studies [8]. Absorption in the SW-NIR region is due to combinations and overtones of vibration such as the stretching and bending of hydrogen-bearing functional groups including –CH, -OH and –NH [9]. Water, melanin, and bilirubin in animals were absorbed by the radiation of this region [8]. In addition, oxyhemoglobin, deoxyhemoglobin, and oxidized cytochrome c oxidase have characteristic absorption spectra in the SW-NIR region [10]. Recently, biologically important molecules such as albumin [11-13], cholesterol [14, 15], globulin [11-13], glucose [13, 16-24], protein [12, 15, 25-28], urea [12, 13, 27], lipid [15], linoleic acid [15], collagen [15], DNA [15], and α-elastin [15] have also been investigated by Vis-NIR spectroscopy. However, there has been considerable debate as to whether the accuracy and stability of Vis-NIR calibration models for non-invasive transcutaneous monitoring of blood glucose levels in patients with diabetes met criteria for clinical diagnosis [18, 29, 30]. Creatine [27], lactate [22, 31], triacetin [20], triglyceride [13], β-lipoprotein [25], Vibrio cholerae [32], Escherichia coli [33, 34], Yeast [35, 36], Ethanol [36, 37], RNA [28], Acetate [34], Ammonia [22, 34], Glycerol [34], and Glutamine [22] have also been quantitatively determined by Vis-NIR spectroscopy. Representative biomolecules studied by Vis-NIR spectroscopy are listed in Table 1.

Vis-NIR spectroscopy has been recognized as having diagnostic potential ever since Jöbsis first used it to demonstrate oxygenation in cats [38]. Vis-NIR spectroscopy has also been applied in the clinical setting to aging [39, 40], Alzheimer's disease [41], cancer [42-50], chronic fatigue syndrome [51-54], dermatological conditions [43], diabetes [18, 21, 55], epilepsy [56], human immunodeficiency virus (HIV) infection [57], seizure types [58], migraine [59], cervical dysplasia [60], atherosclerotic plaques [61], rheumatoid arthritis [62], hemodynamics [63], glioma [64], intraocular pressure [65], hemorrhagic shock [66], skin moisture [67], brain edema [68], optic neuritis [69], and maternal hypotension [70] (Table 2). The number of diseases studied by Vis-NIR spectroscopy has been increasing, although most studies have focused on the monitoring of oxyhemoglobin and deoxyhemoglobin. At present, the diagnostic application of this method in the medical field is rare.

The development of laboratory instrumentation for Vis-NIR spectroscopy has been well reviewed [71]. Manufacturers and commercially available instrumentation has also been listed [72], and the number of manufacturers has shown further dramatic increase. The range of wavelengths and modes of measurement available must be paid greater attention to select a suitable instrument for analysis.

Cuvettes are sometimes used for measurements. Quartz and polystyrene cuvettes are preferable because much Vis-NIR spectral information on quartz and polystyrene has been reported.

The methods of measurement are divided into four types: transmission, reflection, transflection, and interactance in spectroscopy [73]. In transmission spectroscopy, radiation transmitted through sample is measured. In reflection spectroscopy, radiation reflected on the surface is measured. In transflection spectroscopy, which is a combination of the transmission and reflection methods, radiation is transmitted through the sample and scattered back from a reflector on the opposite side. In interactance spectroscopy, radiation transmitted through the sample is collected in contact with the surface of the sample with the end of a fibre optic probe, which has both a radiator and a detector [74]. The availability of fibre optic probes is one advantage of Vis-NIR spectroscopy. Vis-NIR spectroscopy enables the rapid, non-destructive, accurate, and simultaneous determination of multiple components in both liquid and solid samples [75]. However, it also has disadvantages.

(continued on page 10)

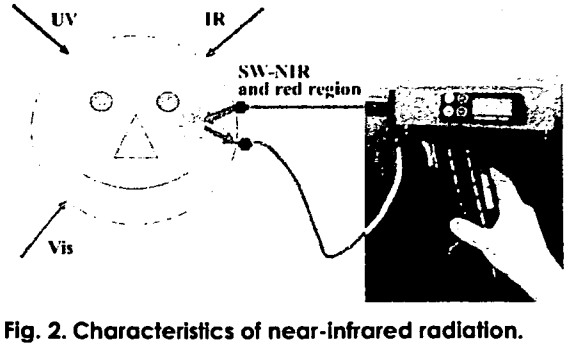

Fig. 2. Characteristics of near-infrared radiation. Ultraviolet (UV), visible (Vis), and infrared (IR) radiation is highly absorbed, whereas near-infrared (NIR) radiation is relatively little absorbed, by water and haemoglobin. Notably, 600-1,100 nm including the red region and short wavelength region of near-infrared (SW-NIR) radiation is called the "optical window", because this region is suitable for biological analysis. Modified from Fig. 1 in Sakudo et al. [103] with permission from Nippon Rinsho Co.

Visible and near-infrared (Vis-NIR) spectroscopy: Introduction and Perspectives for Diagnosis of CFS

Table.1 Representative biomolecules studied by Vis-NIR spectroscopy

Biomolecule	Wavelength [nm]	Algorithm	Reference
Albumin	1300-1850	PLS	[11]
Albumin	400-2500	PLS.MLR	[12]
Albumin	400-2500	PLS.MLR	[13]
Cholesterol	1200-2400	MLR	[14]
Creatine	400-2500	PLS, MLR	[27]
Cytochrome c oxidase	605, 620, 760, 830	None	[87]
Cytochrome c oxidase	700, 730, 750, 805	None	[88]
Cytochrome c oxidase	605, 620, 780, 830	None	[89]
Cytochrome c oxidase	700-865	None	[38]
Globulin	400-2500	PLS.MLR	[12]
Globulin	400-2500	PLS.MLR	[13]
Globulin	1300-1850	PLS	[11]
Glucose	400-2500	PLS.MLR	[13]
Glucose	833-2500	PLS	[16]
Glucose	2000-2500	PLS	[17]
Glucose	400-1700	PLS	[18]
Glucose	2000-2500	PLS	[19]
Glucose	2000-2500	PLS	[20]
Glucose	750-1300	PLS, PCRA	[21]
Hemoglobin	700, 730, 750	None	[90]
Hemoglobin	460-760	Least squares method	[91]
Hemoglobin	700-865	None	[38]
HIV	600-1000	PLS	[57]
Lactate	1000-2500	PLS	[31]
Nitric oxide	470-760	Least squares method	[91]
Prion protein	400-2500	PCA, SIMCA	[92]
Protein	400-2500	PLS.MLR	[12]
Protein	1000-2500	MLR.PCRA.PLS	[25]
Protein	1440-2350	MLR.PCRA.PLS	[26]
Protein	400-2500	PLS, MLR	[27]
RNase A	1250-2500	None	[93]
Triacetin	2000-2500	PLS	[20]
Triglyceride	400-2500	PLS.MLR	[13]
Urea	400-2500	PLS.MLR	[12]
Urea	400-2500	PLS.MLR	[13]
Urea	400-2500	PLS, MLR	[27]
β-lipoprotein	1000-2500	MLR.PCRA.PLS	[25]

Table 1. Representative biomolecules studied by Vis-NIR spectroscopy

HIV: human immunodeficiency virus
MLR: multiple linear regression analysis
PCA: principal component analysis
PCRA: principal component regression analysis
PLS: partial least squares regression analysis
SIMCA: software-independent modeling by class analogy

Vis-NIR spectroscopy is not very sensitive: the limit is only about 0.15% (w/w) for most constituents, and the signal to noise ratio of the instrument is low [less than 10^{-4} optical density (OD)] [76], but is dependent on several factors such as the measurement accessory, spectrometer including detectors, and acquisition time. A large amount of sample is needed for Vis-NIR spectroscopy compared to other methods of chemical analysis [76]. The direct interpretation of spectral absorbance is very difficult for complex mixtures because of broad overlapping and interacting absorption bands [76]. Vis-NIR spectroscopy thus relies on a multivariate analysis to quantify properties or constituents of interest.

A multivariate analysis is an analysis of data with many variables based on statistics and mathematics. It can simplify complicated data and uncover hidden information. The analysis can be qualitative or quantitative. It is based on chemometrics algorithms. Methods of quantitative analysis include the partial least squares regression analysis (PLS) and the principal component regression analysis (PCRA), which are used to develop the regression model for the prediction of the reference value [77, 78]. Methods of qualitative analysis include the principal component analysis (PCA) [79] and the software-independent modeling by class analogy (SIMCA) [80]. PCA is a method for transforming an original variable such as absorbance at various wavelengths into new variables called principal components (PCs). By plotting the data defined by PCs, important relationships in the data (e.g., similarities and differences among objects) can be clearly identified. SIMCA is a recently developed method based on PCA [81]. PCA reduces the amount of data, and SIMCA further extracts discriminant rules among different groups. PCRA is a method for performing PCA on x variables such as wavelength and then regressing y variables on the principal components, whereas PLS

(continued on page 11)

Visible and near-infrared (Vis-NIR) spectroscopy: Introduction and Perspectives for Diagnosis of CFS

Table.2 Representative clinical applications of Vis-NIR spectroscopy

Clinical application	Sample	Biomolecule	Wavelength [nm]	Algorithm	Reference
Aging	Forehead	HbO_2, Hb	775, 825, 850, 904	None	[39]
Alzheimer's disease	Forehead	HbO_2, Hb	775, 825, 850, 904	None	[41]
Atherosclerotic occlusive disease	Posterolateral calf	HbO_2, Hb	700, 750, 830	None	[94]
Biliary anemia	Feces	Bilirubin, Fat	600-2500	Least squares regression analysis	[95]
Breast cancer	Breast tissue	Not identified	625-1050	PCA	[42]
Chronic fatigue syndrome	Gastrocnemius muscle	HbO_2, Hb	760, 850	None	[51]
Chronic fatigue syndrome	Forehead	HbO_2, Hb	780, 805, 830	None	[52]
Chronic fatigue syndrome	Leg	HbO_2, Hb	760, 850	None	[53, 54]
Epilepsy	Forehead	HbO_2, Hb	780, 830	None	[56]
Friedrich's ataxia	Gastrocnemius muscle	HbO_2, Hb	760, 850	None	[96]
HIV infection	Plasma	Not identified	600-1000	PLS	[57]
Lung disease	Forehead	HbO_2, Hb	775, 810, 850, 910	None	[97]
Metabolic myopathies	Gastrocnemius muscle	HbO_2, Hb	760, 850	None	[98]
MELAS and MERRF syndrome	Gastrocnemius muscle	HbO_3, Hb	760, 850	None	[99]
Pigmented and non-pigmented skin	Skin	Not identified	400-2500	PCA	[100]
Schizophrenia	Forehead	HbO_2, Hb	780, 805, 830	None	[101]
Seizure types	Forehead	HbO_2, Hb	730, 810	None	[58]
Skin cancer	Skin	Not identified	400-2500	LDA, Paired t test, Repeated measures analysis of variance	[43, 44]
Type1-diabetes	Finger	Not identified	600-1300	PLS, PCRA	[21]
Type1-diabetes	Thumb	Not identified	400-1700	PLS	[18]
Type2-diabetes	Gastrocnemius muscle	HbO_2, Hb	733, 809	None	[55]
Valvular heart disease	Forehead	HbO_2, Hb	775, 810, 850, 910	None	[102]

Table 2. Representative clinical applications of Vis-NIR spectroscopy

Hb: deoxyhemoglobin
HbO_2: oxyhemoglobin
HIV: Human immunodeficiency virus
LDA: linear discriminant analysis
MELAS: myopathy, encephalopathy, lactic acidosis, and stroke-like episodes
MERRF: myoclonic epilepsy with ragged red fibers
PCA: principal component analysis
PCRA: principal component regression analysis
PLS: partial least squares regression analysis

gives extra weight to variables that show a high correlation with y variables.
Therefore, PLS is usually more effective for predictions than PCR. Further detailed illustrations and mathematical formulas of algorithms are available in many reports about chemometrics [82, 83].

In a multivariate analysis, the number of PCs is important, because too few or too many PCs distort signals or diminish the signal-to-noise ratio, respectively. To choose the correct number of PCs, a validation step is usually included in the process of modeling [9]. For validation steps, internal validation or external validation is used. Most chemometrics software programs include internal cross validation. In internal cross validation, the sample set is repeatedly divided into two groups. One group is reserved for validation and the other, for calibration. This process is repeated until all groups have been used for validation once. In external validation, sample sets are first separated into calibration samples and test samples, which are subjected to validation and used for assessment of the calibration model. By finding the number of PCs when the model shows a minimum standard error of validation (SECV), the number of PCs can be used to describe the signal in the data.

These results suggest that combining Vis-NIR spectroscopy with chemometrics is a promising way to objectively diagnose CFS. They also suggest that an unknown factor or factors present in the serum of all CFS patients could provide important clues as to the agent causing this debilitating disease.

Recently, commercially available chemometrics software programs such as Pirouette (Infometrics, Woodinville, Washington, USA) and Unscrambler (CAMO Inc., Woodbridge, New Jersey, USA) have been used for Vis-NIR analyse. The number of manufacturers of these software programs is increasing. The programs and their manufacturers are listed in Table 3. The software programs are designed to analyze spectral data, and because pre-processing such as standard normal variate (SNV) [84] and smoothing [85], which minimize differences between spectra caused by baseline shifts and noise, is carried out during the analysis, pre-processing handling, which is time-

(continued on page 12)

Visible and near-infrared (Vis-NIR) spectroscopy: Introduction and Perspectives for Diagnosis of CFS (continued)

Table 3. Representative chemometrics software and statistical analysis used in Vis-NIR spectroscopy studies

Name	Manufacturer	Statistical algorithm	
		Regression analysis	Classification methods
Unscrambler	CAMO Inc.	MLR, PCR, PLS	PCA, SIMCA
Pirouette	Infometrics	PCR, PLS, CLS	PCA, HCA, KNN, SIMCA
CharmWorks	Process Analysis and Automation Ltd.	PLS	PCA, SIMCA
Extract	Extract Information AB	PLS	PCA
SIMCA-P	Umetrics		SIMCA
PLS Toolbox	Eigenvector Research Inc.	PLS, PCR	SIMCA, KNN
Sirius	Pattern Recognition Systems	PCR, PLS	PCA
Chemometrics Toolbox	The MathWorks	PCR, PLS	PCA

Table 3. Reprentative chemometrics software and statistical analysis used in Vis-NIR spectroscopy studies

MLR: Mutilinear regression
PCR: Principal component regression
PLS: Partial least squares regression
SIMCA: Soft independent modeling of class analogy
PCA: Principal component analysis
HCA: Hierarchical cluster analysis
KNN: K-nearest neighbors
CLS: Class least squares

consuming, is not required. Furthermore, cross validation steps are also included, and these reduce the overall handling and risk of error during analysis.

Application of Vis-NIR spectroscopy for CFS research

Several biochemical changes are reported in CFS patients, but there is no clear consensus for any of them. Therefore, the diagnosis of CFS is currently based on clinical symptoms. As this approach relies on experience and skill, CFS can be diagnosed only by limited numbers of medical doctors. To overcome these problems, an additional method using instrumentation to achieve an objective diagnosis is needed. We reasoned that Vis-NIR spectroscopy might provide new insights if patients could be compared with individuals without the disorder. Here, we describe the results obtained when sera from CFS patients as well as healthy volunteers were subjected to Vis-NIR spectroscopy [86]. At the Medical Hospital of Osaka City University, serum samples from 77 CFS patients (33.0 ± 8.8 years old; Male/Female: 29/48), diagnosed on the basis of clinical criteria proposed by CDC were examined [1]. Samples from 71healthy volunteers (41.7 ± 10.4 years old; Male/Female: 33/38) were also used. The sera of the 77 CFS patients and 71 healthy volunteers served as test samples to develop calibration models for PCA and SIMCA. Another 99 determinations [54 in the healthy group (35.9 ± 9.1 years old; Male/Female: 11/7) and 45 in CFS patients (34.9 ± 7.0 years old; Male/Female: 8/7)] were masked and used for predictions. All samples were diluted 10-fold with phosphate-buffered saline and adjusted to a constant volume (2 ml) in a polystyrene cuvette before the Vis-NIR spectroscopic measurements. Three consecutive Vis-NIR spectra were measured at a resolution of 2 nm with an NIRGUN (Japan Fantec Research Institute, Shizuoka, Japan) at 37°C. The spectral data were collected as absorbance values [log(1/*T*)], where *T*= transmittance in the wavelength range from 600 to 1,100 nm. Pirouette software (ver. 3.11; Infometrics) was employed for all data processing. To minimize differences between spectra caused by baseline shifts and noise, prior to calibration, spectral data were mean-centered and transformed by SNV [84] and smoothing based on the Savitsky-Golay algorithm [85]. To identify the predominant absorbance peaks in the spectra, PCA and SIMCA methods were further applied to develop PCA and SIMCA models for CFS diagnosis. A clear difference in the sera of CFS patients from those of healthy donors was seen in PCA scores using the first principal component (PC1) and second principal component (PC2) (Fig. 3A, B). The SIMCA model allowed correct separation of the Vis-NIR spectra of 209 of 213 (98.1%) healthy volunteers and 220 of 231 (95.2%) CFS patients. SIMCA using Coomans plots demonstrated that classes of sera from the volunteers and patients did not share multivariate space, providing validation for the separation (Fig. 4A, C). Furthermore, masked samples were subjected to Vis-NIR spectroscopy, and predictions made with the PCA and SIMCA models. PCA clearly distinguished the masked samples of the healthy volunteers from those of the CFS patients (Fig. 3C). SIMCA correctly predicted 54 of 54 (100%) volunteers and 42 of 45 (93.3%) patients (Fig. 4B, D).

These results suggest that combining Vis-NIR spectroscopy with chemometrics is a promising way to objectively diagnose CFS. They also suggest that an unknown factor or factors present in the serum of all CFS patients could provide important clues as to the agent causing this debilitating disease.

We concede that statistically, the results are not robust enough for clinical use at this time. The PCA and SIMCA model was developed from Vis-NIR

(continued on page 13)

Visible and near-infrared (Vis-NIR) spectroscopy: Introduction and Perspectives for Diagnosis of CFS (continued)

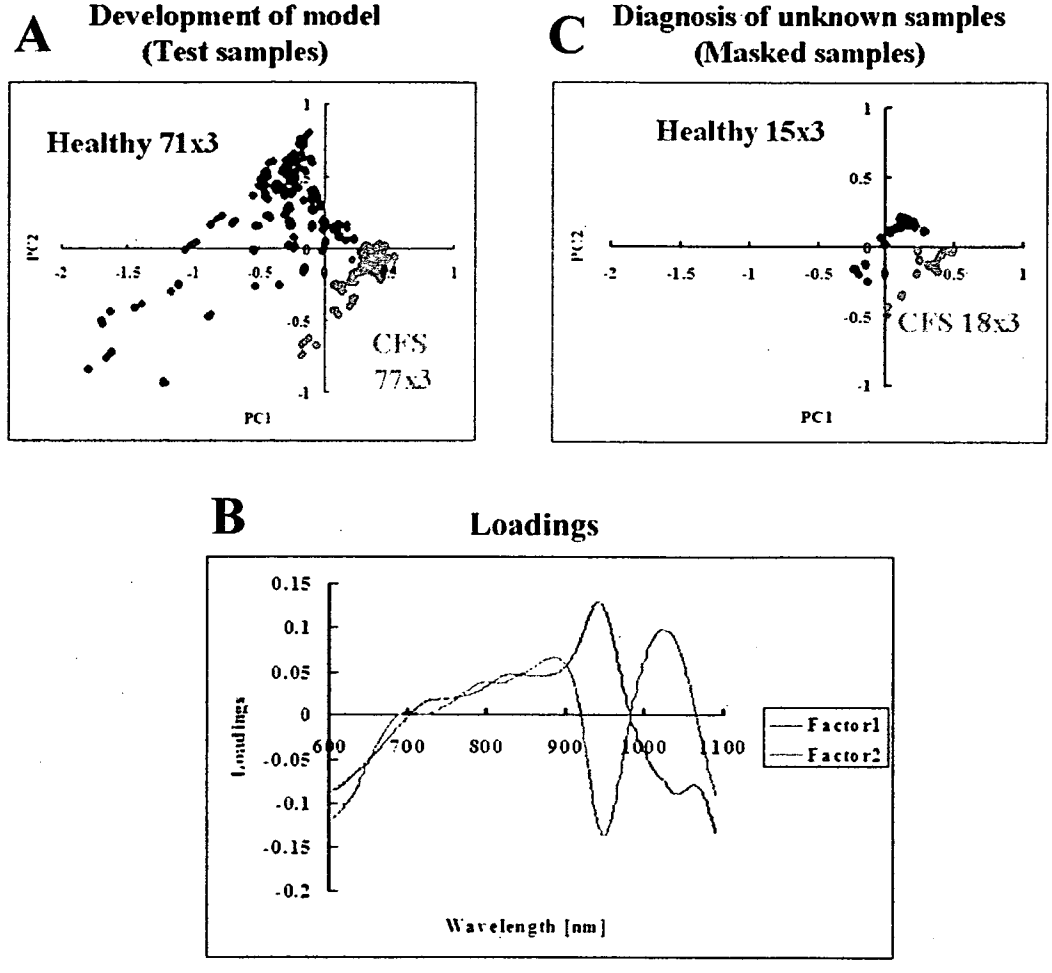

Fig. 3. PCA of Vis-NIR spectra of serum samples for CFS diagnosis

(A-B) Vis-NIR spectra of serum samples from healthy donors (Blue) and CFS patients (Red) were subjected to PCA and the results plotted as PC1 *versus* PC2 to establish a PCA model (A). Loadings show the importance of each wavelength for the PCs indicated by peaks (B). (C) Masked samples, which were not used for development of the model, were subjected to PCA and the results plotted as PC1 *versus* PC2. Modified from Fig. 1 in Sakudo et al. [86] with permission from Elsevier.

spectra of 148 individuals including 77 CFS patients and 71 healthy donors, not a sufficient number for practical use in the clinic. The influences of sex and race, etc. on the results of this diagnostic method remain unclear. To obtain more Vis-NIR spectra, samples for the calibration set should be obtained in a similar way to those that will be analyzed for diagnosis. Furthermore, uniformity of the solvent among samples is very important. For example, in blood samples, identical methods of preparation of serum are necessary.

Stable humidity and temperature should be maintained during the scanning event, because humidity and temperature may affect water absorption in the NIR region. In this study, we used serum samples for Vis-NIR spectroscopy. Therefore, the method is invasive but non-destructive. Vis-NIR spectroscopy can also be applied to non-invasive analyse and we are now approaching the non- invasive diagnosis of CFS (Fig. 5).Hopefully, after these issues are addressed, this diagnostic method might be adopted in the clinic (Fig 6).

The next step in terms of research into the disease, as opposed to diagnosis, is to use this approach together with other evidence to try and identify specific biochemical markers common to CFS. This is the best way to understand the cause of CFS. Our experimental system coupling Vis-NIR spectroscopy with chemometrics may also contribute to this issue.

Finally, we would like to emphasize that international collaboration is important in the development of this method, because CFS is heterogeneous and diagnostic criteria differ slightly among countries. Differences and similarities between CFS and CFS-like diseases such as ME, PVFS, CFIDS, and 'Yuppie flu' would also be made clear by this method.

(continued on page 14)

Visible and near-infrared (Vis-NIR) spectroscopy: Introduction and Perspectives for Diagnosis of CFS (continued)

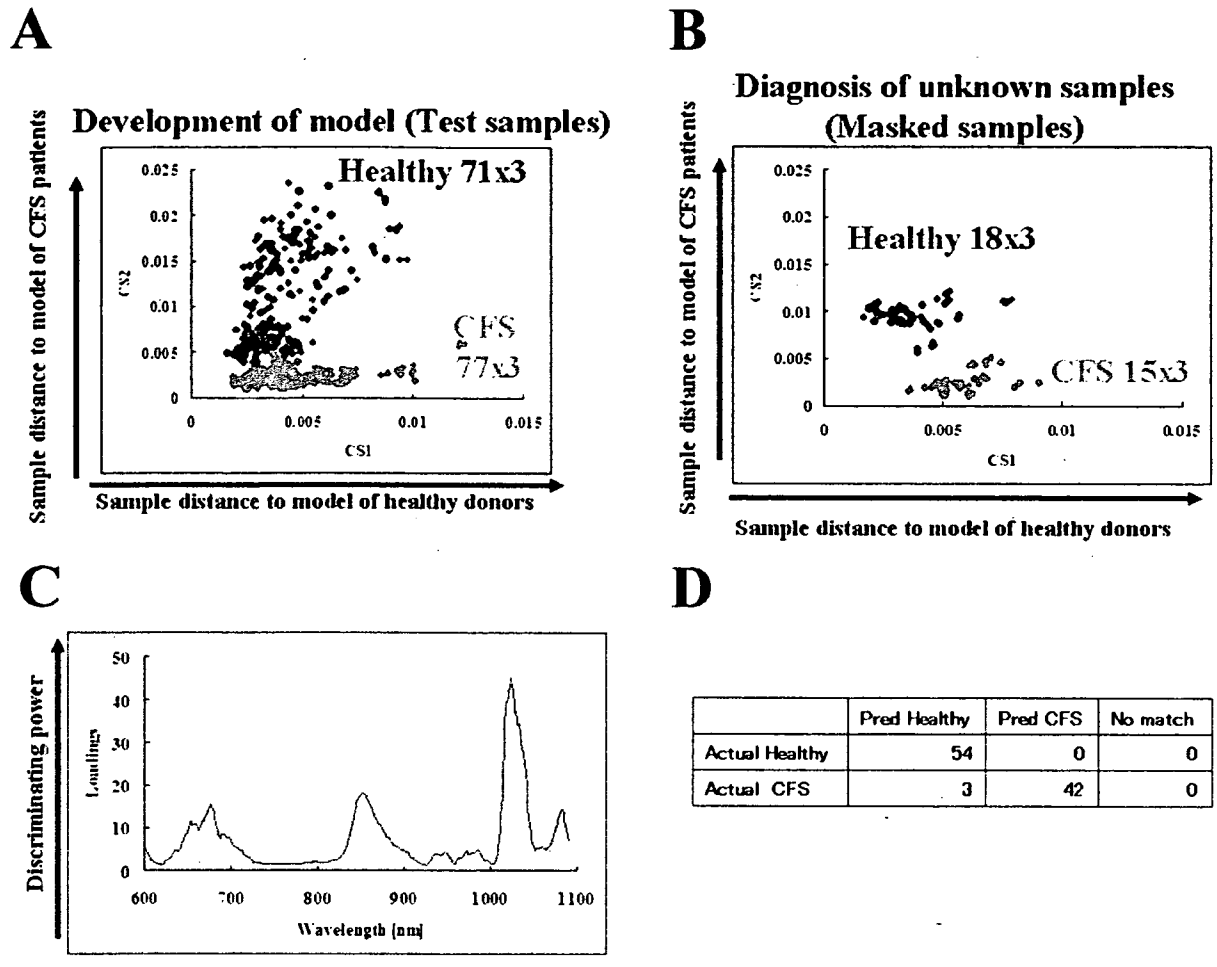

	Pred Healthy	Pred CFS	No match
Actual Healthy	54	0	0
Actual CFS	3	42	0

Fig. 4. SIMCA analysis of Vis-NIR spectra of serum samples for CFS diagnosis

(A-B) Vis-NIR spectra of serum samples from healthy donors (Blue) and CFS patients (Red) were subjected to SIMCA. Coomans plots show distances to model of healthy donors *versus* CFS patients to establish a SIMCA model (A). Discriminating power shows the importance of each wavelength for distinguishing healthy donors from CFS patients (B). (C) Masked samples, which were not used for development of the model, were subjected to SIMCA. Coomans plots show distances to model of healthy donors *versus* CFS patients. Modified from Fig. 2 in Sakudo et al. [86] with permission from Elsevier.

References

[1] K. Fukuda, S.E. Straus, I. Hickie, M.C. Sharpe, J.G. Dobbins, and A. Komaroff, The chronic fatigue syndrome: a comprehensive approach to its definition and study. International Chronic Fatigue Syndrome Study Group. Ann Intern Med 121 (1994) 953-9.

[2] L.A. Jason, J.A. Richman, A.W. Rademaker, K.M. Jordan, A.V. Plioplys, R.R. Taylor, W. McCready, C.F. Huang, and S. Plioplys, A community-based study of chronic fatigue syndrome. Arch Intern Med 159 (1999) 2129-37.

[3] H. Kuratsune, Overview of chronic fatigue syndrome focusing on prevalence and diagnostic criteria. Nippon Rinsho 65 (2007) 983-90.

[4] K.J. Reynolds, S.D. Vernon, E. Bouchery, and W.C. Reeves, The economic impact of chronic fatigue syndrome. Cost Eff Resour Alloc 2 (2004) 4.

[5] M. Reyes, R. Nisenbaum, D.C. Hoaglin, E.R. Unger, C. Emmons, B. Randall, J.A. Stewart, S. Abbey, J.F. Jones, N. Gantz, S. Minden, and W.C. Reeves, Prevalence and incidence of chronic fatigue syndrome in Wichita, Kansas. Arch Intern Med 163 (2003) 1530-6.

[6] S.D. Vernon, T. Whistler, E. Aslakson, M. Rajeevan, and W.C. Reeves, Challenges for molecular profiling of chronic fatigue syndrome. Pharmacogenomics 7 (2006) 211-8.

(continued on page 15)

Visible and near-infrared (Vis-NIR) spectroscopy: Introduction and Perspectives for Diagnosis of CFS (continued)

[7] S. Nioka, and B. Chance, NIR spectroscopic detection of breast cancer. Technol Cancer Res Treat 4 (2005) 497-512.
[8] K. Konig, Multiphoton microscopy in life sciences. J Microsc 200 (2000) 83-104.
[9] I. Murray, Forage analysis by near infra-red spectroscopy, in: A. Davies, R.D. Baker, S.A. Grant (Eds.), Sward Management Handbook, British Grassland Society, UK, 1993, pp. 285-312.
[10] B.L. Horecker, The absorbance spectra of hemoglobin and its derivatives in the visible and near infra-red regions. J Biol Chem 148 (1973) 173-83.
[11] K. Murayama, K. Yamada, R. Tsenkova, Y. Wang, Y. Ozaki, Near-infrared spectra of serum albumin and gamma-globulin and determination of their concentrations in phosphate buffer solutions by partial least squares regression. Vib Spectrosc 18 (1998) 33-40.
[12] J.W. Hall, and A. Pollard, Near-infrared spectroscopic determination of serum total proteins, albumin, globulins, and urea. Clin Biochem 26 (1993) 483-90.
[13] J.W. Hall, and A. Pollard, Near-infrared spectrophotometry: a new dimension in clinical chemistry. Clin Chem 38 (1992) 1623-31.
[14] E. Peuchant, C. Salles, and R. Jensen, Determination of serum cholesterol by near-infrared reflectance spectrometry. Anal Chem 59 (1987) 1816-9.
[15] N. Hirosawa, Y. Sakamoto, H. Katayama, S. Tonooka, and K. Yano, In vivo investigation of progressive alterations in rat mammary gland tumors by near-infrared spectroscopy. Anal Biochem 305 (2002) 156-65.
[16] H.M. Heise, R. Marbach, T. Koschinsky, and F.A. Gries, Noninvasive blood glucose sensors based on near-infrared spectroscopy. Artif Organs 18 (1994) 439-47.
[17] L.A. Marquardt, M.A. Arnold, and G.W. Small, Near-infrared spectroscopic measurement of glucose in a protein matrix. Anal Chem 65 (1993) 3271-8.
[18] I. Gabriely, R. Wozniak, M. Mevorach, J. Kaplan, Y. Aharon, and H. Shamoon, Transcutaneous glucose measurement using near-infrared spectroscopy during hypoglycemia. Diabetes Care 22 (1999) 2026-32.
[19] G.W. Small, M.A. Arnold, and L.A. Marquardt, Strategies for coupling digital filtering with partial least-squares regression: application to the determination of glucose in plasma by Fourier transform near-infrared spectroscopy. Anal Chem 65 (1993) 3279-89.
[20] S. Pan, H. Chung, M.A. Arnold, and G.W. Small, Near-infrared spectroscopic measurement of physiological glucose levels in variable matrices of protein and triglycerides. Anal Chem 68 (1996) 1124-35.
[21] M.R. Robinson, R.P. Eaton, D.M. Haaland, G.W. Koepp, E.V. Thomas, B.R. Stallard, and P.L. Robinson, Noninvasive glucose monitoring in diabetic patients: a preliminary evaluation. Clin Chem 38 (1992) 1618-22.
[22] S.A. Arnold, J. Crowley, N. Woods, L.M. Harvey, and B. McNeil, In-situ near infrared spectroscopy to monitor key analytes in mammalian cell cultivation. Biotechnol Bioeng 84 (2003) 13-9.
[23] K. Maruo, M. Tsurugi, M. Tamura, and Y. Ozaki,

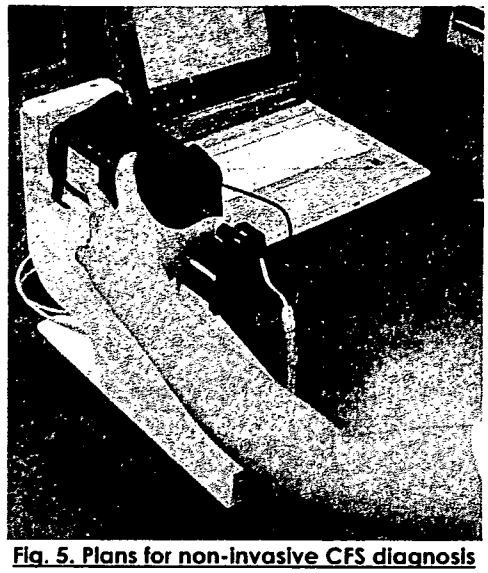

Fig. 5. Plans for non-invasive CFS diagnosis using Vis-NIR spectroscopy

Vis-NIR spectroscopy can be used for non-invasive analyse, because Vis-NIR is highly transmissible into the body. Now, we are trying to study the potential of Vis-NIR spectra collected from the thumb for the diagnosis of CFS. Modified from Fig. 5 in Sakudo et al. [103] with permission from Nippon Rinsho Co.

In vivo noninvasive measurement of blood glucose by near-infrared diffuse-reflectance spectroscopy. Appl Spectrosc 57 (2003) 1236-44.
[24] H.M. Heise, A. Bittner, R. Marbach, Clinical chemistry and near infrared spectroscopy: technology for non-invasive glucose monitoring. J Near Infrared Spectrosc 6 (1998) 349-59.
[25] G. Domján, K.J. Kaffka, J.M. Jáko, I.T. Vályi-Nagya, Rapid analysis of whole blood and blood serum using near infrared spectroscopy. J Near Infrared Spectrosc 2 (1995) 67-78.
[26] A.W. van Toorenenbergen, B.G. Blijenberg, and B. Leijnse, Measurement of total serum protein by near-infrared reflectance spectroscopy. J Clin Chem Clin Biochem 26 (1988) 209-11.
[27] R.A. Shaw, S. Kotowich, H.H. Mantsch, and M. Leroux, Quantitation of protein, creatinine, and urea in urine by near-infrared spectroscopy. Clin Biochem 29 (1996) 11-19.
[28] K.S. Yeung, M. Hoare, N.F. Thornhill, T. Williams, and J.D. Vaghjiani, Near-infrared spectroscopy for bioprocess monitoring and control. Biotechnol Bioeng 63 (1999) 684-93.
[29] H.M. Heise, and P. Lampen, Transcutaneous glucose measurements using near-infrared spectroscopy: validation of statistical calibration models. Diabetes Care 23 (2000) 1208-10.

(continued on page 16)

Visible and near-infrared (Vis-NIR) spectroscopy: Introduction and Perspectives for Diagnosis of CFS (continued)

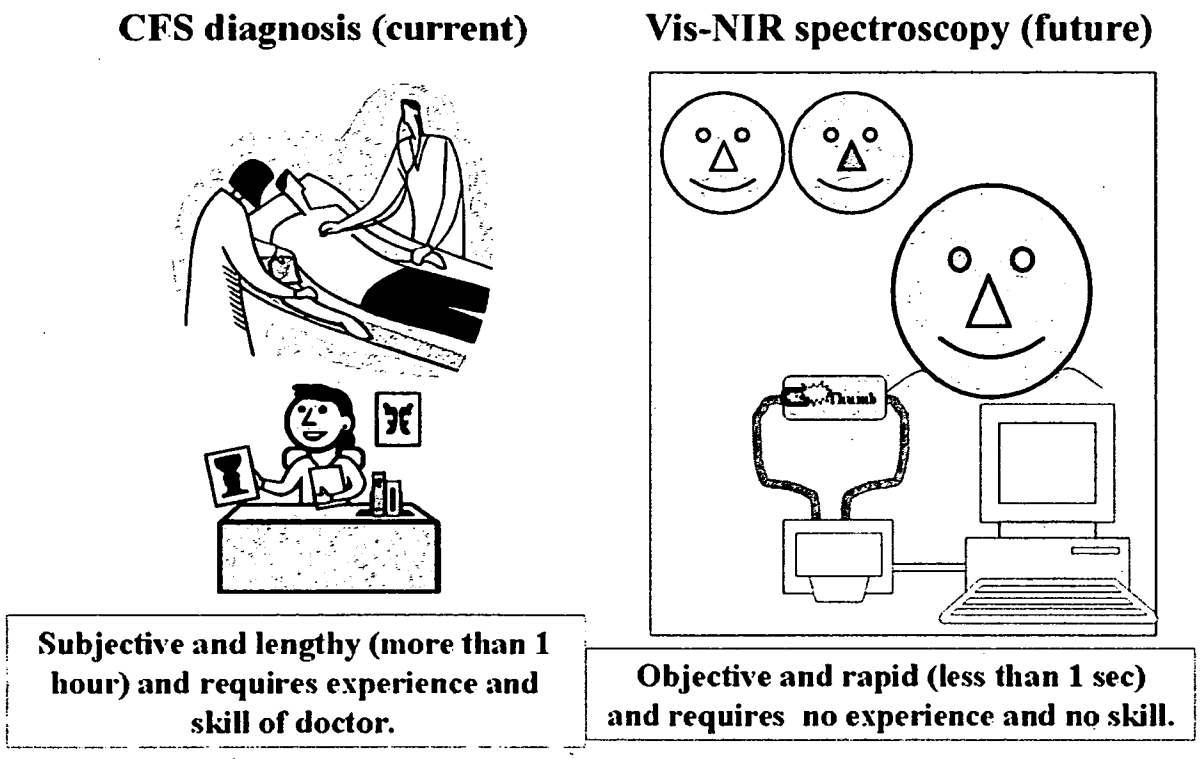

Fig. 6. Comparison of current CFS diagnosis and future Vis-NIR CFS diagnosis
Currently, CFS can only be diagnosed by skilled doctors. The diagnosis requires experience and sophisticated techniques. Furthermore, even with a skilled doctor, it takes long time to reach a final clinical diagnosis. Vis-NIR spectroscopy would enable an objective and rapid diagnosis. Moreover, it would not require experience and skill. Modified from Fig. 2 in Sakudo et al. [103] with permission from Nippon Rinsho Co.

[30] H.M. Heise, Applications of near-infrared spectroscopy in medical sciences, in: H.W. Siesler, Y. Ozaki, S. Kawata (Eds.), Near-infrared spectroscopy (Principles, instruments, applications), Wiley-VCH, Weinheim, 2002, pp. 289-333.
[31] D. Lafrance, L. Lands, D. Burns, In vivo lactate measurement in human tissue by near-infrared diffuse reflectance spectroscopy. Vib Spectrosc 36 (2004) 195-202.
[32] M. Navratil, A. Norberg, L. Lembren, and C.F. Mandenius, On-line multi-analyzer monitoring of biomass, glucose and acetate for growth rate control of a Vibrio cholerae fed-batch cultivation. J Biotechnol 115 (2005) 67-79.
[33] S.A. Arnold, R. Gaensakoo, L.M. Harvey, and B. McNeil, Use of at-line and in-situ near-infrared spectroscopy to monitor biomass in an industrial fed-batch Escherichia coli process. Biotechnol Bioeng 80 (2002) 405-13.
[34] J.W. Hall, B. McNeil, M.J. Rollins, I. Draper, B.G. Thompson, G. Macaloney, Near-infrared spectroscopic determination of acetate, ammonium, biomass, and glycerol in an industrial Escherichia coli fermentation. Appl Spectrosc 50 (1996) 102-8.
[35] R.P. Kasprow, A.J. Lange, and D.J. Kirwan, Correlation of fermentation yield with yeast extract composition as characterized by near-infrared spectroscopy. Biotechnol Prog 14 (1998) 318-25.
[36] M. Blanco, A.C. Peinado, and J. Mas, Analytical monitoring of alcoholic fermentation using NIR spectroscopy. Biotechnol Bioeng 88 (2004) 536-42.
[37] A.G. Cavinato, D.M. Mayes, Z.H. Ge, and J.B. Callis, Noninvasive method for monitoring ethanol in fermentation processes using fiber-optic near-infrared spectroscopy. Anal Chem 62 (1990) 1977-82.
[38] F.F. Jobsis, Noninvasive, infrared monitoring of cerebral and myocardial oxygen sufficiency and circulatory parameters. Science 198 (1977) 1264-7.
[39] C. Hock, F. Muller-Spahn, S. Schuh-Hofer, M. Hofmann, U. Dirnagl, and A. Villringer, Age dependency of changes in cerebral hemoglobin oxygenation during brain activation: a near-infrared spectroscopy study. J Cereb Blood Flow Metab 15 (1995) 1103-8.
[40] A.E. Cerussi, A.J. Berger, F. Bevilacqua, N. Shah, D. Jakubowski, J. Butler, R.F. Holcombe, and B.J. Tromberg, Sources of absorption and scattering contrast for near-infrared optical mammography. Acad Radiol 8 (2001) 211-8.
[41] C. Hock, K. Villringer, F. Muller-Spahn, M. Hofmann, S. Schuh-Hofer, H. Heekeren, R. Wenzel, U. Dirnagl, and A. Villringer, Near infrared spectroscopy in the diagnosis of Alzheimer's disease. Ann N Y Acad Sci 777 (1996) 22-9.

(continued on page 17)

Visible and near-infrared (Vis-NIR) spectroscopy: Introduction and Perspectives for Diagnosis of CFS (continued)

[42] M.K. Simick, R. Jong, B. Wilson, and L. Lilge, Non-ionizing near-infrared radiation transillumination spectroscopy for breast tissue density and assessment of breast cancer risk. J Biomed Opt 9 (2004) 794-803.
[43] L.M. McIntosh, R. Summers, M. Jackson, H.H. Mantsch, J.R. Mansfield, M. Howlett, A.N. Crowson, and J.W. Toole, Towards non-invasive screening of skin lesions by near-infrared spectroscopy. J Invest Dermatol 116 (2001) 175-81.
[44] L. McIntosh, M. Jackson, H.H. Mantsch, J.R. Mansfield, A.N. Crowson, J.W.P. Toole, Near-infrared spectroscopy for dermatological applications. Vib Spectrosc 28, 2002, 53-8.
[45] S.B. Colak, M.B. van der Mark, G.W. Hooft, Clinical optical tomography and NIR spectroscopy for breast cancer detection. IEEE J Quantum Electron 5 (1999) 1143-58.
[46] J.H. Ali, W.B. Wang, M. Zevallos, and R.R. Alfano, Near infrared spectroscopy and imaging to probe differences in water content in normal and cancer human prostate tissues. Technol Cancer Res Treat 3 (2004) 491-7.
[47] P. Crow, A. Molckovsky, N. Stone, J. Uff, B. Wilson, and L.M. WongKeeSong, Assessment of fiberoptic near-infrared raman spectroscopy for diagnosis of bladder and prostate cancer. Urology 65 (2005) 1126-30.
[48] H. Yamazaki, S. Kaminaka, E. Kohda, M. Mukai, and H.O. Hamaguchi, The diagnosis of lung cancer using 1064-nm excited near-infrared multichannel Raman spectroscopy. Radiat Med 21 (2003) 1-6.
[49] A. Molckovsky, L.M. Song, M.G. Shim, N.E. Marcon, and B.C. Wilson, Diagnostic potential of near-infrared Raman spectroscopy in the colon: differentiating adenomatous from hyperplastic polyps. Gastrointest Endosc 57 (2003) 396-402.
[50] S.H. Yan, J. Mayaudon J:Near infrared prediction and biochemical properties in human breast invasive carcinoma tissues. J Near Infrared Spectrosc 6, A273-7 (1998).
[51] K.K. McCully, S. Smith, S. Rajaei, J.S. Leigh, Jr., and B.H. Natelson, Muscle metabolism with blood flow restriction in chronic fatigue syndrome. J Appl Physiol 96 (2004) 871-8.
[52] H. Tanaka, R. Matsushima, H. Tamai, and Y. Kajimoto, Impaired postural cerebral hemodynamics in young patients with chronic fatigue with and without orthostatic intolerance. J Pediatr 140 (2002) 412-7.
[53] K.K. McCully, S. Smith, S. Rajaei, J.S. Leigh, Jr., and B.H. Natelson, Blood flow and muscle metabolism in chronic fatigue syndrome. Clin Sci (Lond) 104 (2003) 641-7.
[54] K.K. McCully, and B.H. Natelson, Impaired oxygen delivery to muscle in chronic fatigue syndrome. Clin Sci (Lond) 97 (1999) 603-8; discussion 611-3.
[55] M. Scheuermann-Freestone, P.L. Madsen, D. Manners, A.M. Blamire, R.E. Buckingham, P. Styles, G.K. Radda, S. Neubauer, and K. Clarke, Abnormal cardiac and skeletal muscle energy metabolism in patients with type 2 diabetes. Circulation 107 (2003) 3040-6.
[56] E. Watanabe, Y. Nagahori, and Y. Mayanagi, Focus diagnosis of epilepsy using near-infrared spectroscopy. Epilepsia 43 Suppl 9 (2002) 50-5.
[57] A. Sakudo, R. Tsenkova, T. Onozuka, K. Morita, S. Li, J. Warachit, Y. Iwabu, G. Li, T. Onodera, and K. Ikuta, A novel diagnostic method for human immunodeficiency virus type-1 in plasma by near-infrared spectroscopy. Microbiol Immunol 49 (2005) 695-701.
[58] D.K. Sokol, O.N. Markand, E.C. Daly, T.G. Luerssen, and M.D. Malkoff, Near infrared spectroscopy (NIRS) distinguishes seizure types. Seizure 9 (2000) 323-7.
[59] N. Shinoura, and R. Yamada, Decreased vasoreactivity to right cerebral hemisphere pressure in migraine without aura: a near-infrared spectroscopy study. Clin Neurophysiol 116 (2005) 1280-5.
[60] R. Hornung, T.H. Pham, K.A. Keefe, M.W. Berns, Y. Tadir, and B.J. Tromberg, Quantitative near-infrared spectroscopy of cervical dysplasia in vivo. Hum Reprod 14 (1999) 2908-16.
[61] J. Wang, Y.J. Geng, B. Guo, T. Klima, B.N. Lal, J.T. Willerson, and W. Casscells, Near-infrared spectroscopic characterization of human advanced atherosclerotic plaques. J Am Coll Cardiol 39 (2002) 1305-13.
[62] J.M. Canvin, S. Bernatsky, C.A. Hitchon, M. Jackson, M.G. Sowa, J.R. Mansfield, H.H. Eysel, H.H. Mantsch, and H.S. El-Gabalawy, Infrared spectroscopy: shedding light on synovitis in patients with rheumatoid arthritis. Rheumatology (Oxford) 42 (2003) 76-82.
[63] T. Binzoni, T. Leung, V. Hollis, S. Bianchi, J.H. Fasel, H. Bounameaux, E. Hiltbrand, and D. Delpy, Human tibia bone marrow: defining a model for the study of haemodynamics as a function of age by near infrared spectroscopy. J Physiol Anthropol Appl Human Sci 22 (2003) 211-8.
[64] S. Asgari, H.J. Rohrborn, T. Engelhorn, and D. Stolke, Intra-operative characterization of gliomas by near-infrared spectroscopy: possible association with prognosis. Acta Neurochir (Wien) 145 (2003) 453-59; discussion 459-60.
[65] D. Weissbrodt, R. Mueller, J. Backhaus, and J.B. Jonas, Non-invasive measurement of intraocular pressure by near-infrared spectroscopy. Am J Ophthalmol 140 (2005) 307-8.
[66] J.H. Taylor, K.E. Mulier, D.E. Myers, and G.J. Beilman, Use of near-infrared spectroscopy in early determination of irreversible hemorrhagic shock. J Trauma 58 (2005) 1119-25.
[67] E.J. Suh, Y.A. Woo, and H.J. Kim, Determination of water content in skin by using a FT near infrared spectrometer. Arch Pharm Res 28 (2005) 458-62.
[67] E.J. Suh, Y.A. Woo, and H.J. Kim, Determination of water content in skin by using a FT near infrared spectrometer. Arch Pharm Res 28 (2005) 458-62.
[68] J.R. Thiagarajah, M.C. Papadopoulos, and A.S. Verkman, Noninvasive early detection of brain edema in mice by near-infrar
ed light scattering. J Neurosci Res 80 (2005) 293-9. [69] A. Miki, T. Nakajima, M. Takagi, T. Usui, H. Abe, C.S. Liu, and G.T. Liu, Near-infrared spectroscopy of the visual cortex in unilateral optic neuritis. Am J Ophthalmol 139 (2005) 353-6.
[70] P.A. Berlac, and Y.H. Rasmussen, Per-operative cerebral near-infrared spectroscopy (NIRS) predicts maternal hypotension during elective caesarean delivery in spinal anaesthesia. Int J Obstet Anesth 14 (2005) 26-31.

(continued on page 18)

Visible and near-infrared (Vis-NIR) spectroscopy: Introduction and Perspectives for Diagnosis of CFS (continued)

[71] W.F. McClure, 204 years of near infrared technology: 1800-2003. J Near Infrared Spectrosc 11 (2003) 487-518.
[72] W.F. McClure, Near-infrared spectroscopy: the giant is running strong. Anal Chem 66 (1994) 43A-53A.
[73] S. Kawano, Sampling and sample presentation, in: H.W. Siesler, Y. Ozaki, S. Kawata (Eds.), Near-infrared spectroscopy (Principles, instruments, applications), Wiley-VCH, Weinheim, 2002, 115-24.
[74] J.M. Conway, K.H. Norris, and C.E. Bodwell, A new approach for the estimation of body composition: infrared interactance. Am J Clin Nutr 40 (1984) 1123-30.
[75] E.W. Ciurczak, J.K. Drennen, Pharmaceutical and Medical Applications of Near-Infrared Applications (Pratical Spectroscopy), Marcel Dekker Inc., New York, 2002.
[76] M. Iwamoto, S. Kawano, Advantages and disadvantages of NIR applications for the food industry, in: I. Murray, A.I. Cowe (Eds.), Making light work: advances in near infrared spectroscopy: developed from the 4th International Conference on Near Infrared Spectroscopy, Aberdeen, Scotland, August 19-23, 1991.,VCH, New York, 1992, pp. 367-75.
[77] H. Martens, T. Naes, Multivariate calibration, John Wiley & Sons, Chichester, UK, 1991.
[78] H. Wold H, Partial Least Squares, in: S. Katz, N.L. Johnson (Eds.), Encyclopedia of Statistical Sciences, John Wiley & Sons, New York, 1985, pp. 581-91.
[79] I.T. Jolliffe, Principal component analysis (2nd ed), Springer, New York, 2002.
[80] B.K. Lavine, Clustering and classification of analytical data, in: R.A. Meyers (Ed.), Encyclopedia of analytical chemistry: applications, theory and instrumentation, John Wiley, New York, 2000, pp. 1-21.
[81] S. Wold, Pattern recognition by means of disjoint principal componets models. Pattern Recognit 8 (1976) 127-39.
[82] H.M. Heise, R. Winzen, Chemometrics in near-infrared spectroscopy, principles, instruments, applications, in: H.W. Siesler (Ed.), Near-infrared spectroscopy: principles, instruments, applications, Wiley-VCH, Weinheim, Germany, 2002, pp. 125-62.
[83] J.N. Miller, J.C. Miller, Statistics and chemometrics for analytical chemistry (4th ed.), Prentice Hall, UK, 2000.
[84] R.J. Barnes, M.S. Dhanoa, S.J. Lister, Standard Normal Variate Transformation and De-trending of Near-Infrared Diffuse Reflectance Spectra. Appl Spectrosc 43 (1989) 772-7.
[85] A. Savitzky, M.J.E. Golay, Smoothing and differentiation of data by simplified least-squares procedures. Anal Chem 36 (1964) 1627-39.
[86] A. Sakudo, H. Kuratsune, T. Kobayashi, S. Tajima, Y. Watanabe, and K. Ikuta, Spectroscopic diagnosis of chronic fatigue syndrome by visible and near-infrared spectroscopy in serum samples. Biochem Biophys Res Commun 345 (2006) 1513-6.
[87] Y. Hoshi, O. Hazeki, and M. Tamura, Oxygen dependence of redox state of copper in cytochrome oxidase in vitro. J Appl Physiol 74 (1993) 1622-7.
[88] Y. Hoshi, O. Hazeki, Y. Kakihana, and M. Tamura, Redox behavior of cytochrome oxidase in the rat brain measured by near-infrared spectroscopy. J Appl Physiol 83 (1997) 1842-8.
[89] A. Matsunaga, Y. Nomura, S. Kuroda, M. Tamura, J. Nishihira, and N. Yoshimura, Energy-dependent redox state of heme a + a3 and copper of cytochrome oxidase in perfused rat brain in situ. Am J Physiol 275 (1998) C1022-30.
[90] Y. Hoshi, N. Kobayashi, and M. Tamura, Interpretation of near-infrared spectroscopy signals: a study with a newly developed perfused rat brain model. J Appl Physiol 90 (2001) 1657-62.
[91] F.A. Martin, D. Rojas-Diaz, M.A. Luis-Garcia, J.L. Gonzalez-Mora, and M.A. Castellano, Simultaneous monitoring of nitric oxide, oxyhemoglobin and deoxyhemoglobin from small areas of the rat brain by in vivo visible spectroscopy and a least-square approach. J Neurosci Methods 140 (2004) 75-80.
[92] R.N. Tsenkova, I.K. Iordanova, K. Toyoda, and D.R. Brown, Prion protein fate governed by metal binding. Biochem Biophys Res Commun 325 (2004) 1005-12.
[93] C.P. Schultz, H. Fabian, and H.H. Mantsch, Two-dimensional mid-IR and near-IR correlation spectra of ribonuclease A: using overtones and combination modes to monitor changes in secondary structure. Biospectroscopy 4 (1998) S19-29.
[94] T. Watanabe, M. Matsushita, N. Nishikimi, T. Sakurai, K. Komori, and Y. Nimura, Near-infrared spectroscopy with treadmill exercise to assess lower limb ischemia in patients with atherosclerotic occlusive disease. Surg Today 34 (2004) 849-54.
[95] T. Akiyama, and Y. Yamauchi, Use of near infrared reflectance spectroscopy in the screening for biliary atresia. J Pediatr Surg 29 (1994) 645-7.
[96] D.R. Lynch, G. Lech, J.M. Farmer, L.J. Balcer, W. Bank, B. Chance, and R.B. Wilson, Near infrared muscle spectroscopy in patients with Friedreich's ataxia. Muscle Nerve 25 (2002) 664-73.
[97] G. Jensen, H.B. Nielsen, K. Ide, P.L. Madsen, L.B. Svendsen, U.G. Svendsen, and N.H. Secher, Cerebral oxygenation during exercise in patients with terminal lung disease. Chest 122 (2002) 445-50.
[98] W. Bank, and B. Chance, An oxidative defect in metabolic myopathies: diagnosis by noninvasive tissue oximetry. Ann Neurol 36 (1994) 830-7.
[99] W. Bank, and B. Chance, Diagnosis of defects in oxidative muscle metabolism by non-invasive tissue oximetry. Mol Cell Biochem 174 (1997) 7-10.
[100] R.K. Lauridsen, H. Everland, L.F. Nielsen, S.B. Engelsen, and L. Norgaard, Exploratory multivariate spectroscopic study on human skin. Skin Res Technol 9 (2003) 137-46.
[101] F. Okada, Y. Tokumitsu, Y. Hoshi, and M. Tamura, Impaired interhemispheric integration in brain oxygenation and hemodynamics in schizophrenia. Eur Arch Psychiatry Clin Neurosci 244 (1994) 17-25.
[102] A. Koike, H. Itoh, R. Oohara, M. Hoshimoto, A. Tajima, T. Aizawa, and L.T. Fu, Cerebral oxygenation during exercise in cardiac patients. Chest 125 (2004) 182-90.
[103] A. Sakudo, H. Kuratsune, Y. Hakariya, T. Kobayashi, and K. Ikuta, Spectroscopic diagnosis of chronic fatigue syndrome by multivariate analysis of visible and near-infrared spectra. Nippon Rinsho 65 (2007) 1051-6.

Microbiol. Immunol., 51(1), 1–13, 2007

Minireview

Prion Protein Gene-Deficient Cell Lines: Powerful Tools for Prion Biology

Akikazu Sakudo*[1,2], Takashi Onodera[2], and Kazuyoshi Ikuta[1]

[1]*Department of Virology, Research Institute for Microbial Diseases, Osaka University, Suita, Osaka 565–0871, Japan*
[2]*Department of Molecular Immunology, School of Agricultural and Life Sciences, University of Tokyo, Bunkyo-ku, Tokyo 113–8657, Japan*

Received October 5, 2006

***Abstract*: Prion diseases are zoonotic infectious diseases commonly transmissible among animals *via* prion infections with an accompanying deficiency of cellular prion protein (PrP^C) and accumulation of an abnormal isoform of prion protein (PrP^{Sc}), which are observed in neurons in the event of injury and disease. To understand the role of PrP^C in the neuron in health and diseases, we have established an immortalized neuronal cell line HpL3-4 from primary hippocampal cells of prion protein (PrP) gene-deficient mice by using a retroviral vector encoding Simian Virus 40 Large T antigen (SV40 LTag). The HpL3-4 cells exhibit cell-type-specific proteins for the neuronal precursor lineage. Recently, this group and other groups have established PrP-deficient cell lines from many kinds of cell types including glia, fibroblasts and neuronal cells, which will have a broad range of applications in prion biology. In this review, we focus on recently obtained information about PrP functions and possible studies on prion infections using the PrP-deficient cell lines.**

***Key words*: Prion disease, Apoptosis, Oxidative stress, Prion protein, BSE, Cell line**

Introduction

Transmissible spongiform encephalopathy (TSE) is a zoonotic infectious disease which can be spread by intracerebral, intraperitoneal, and oral infections (40). Forms of TSE include scrapie, transmissible mink encephalopathy (TME), chronic wasting disease (CWD), feline spongiform encephalopathy (FSE), exotic ruminants encephalopathy and bovine spongiform encephalopathy (BSE) (5, 45). Humans are also susceptible to several types of TSE: Creutzfeldt-Jakob disease (CJD), Gerstmann-Sträussler-Scheinker Syndrome (GSS), fatal familial insomnia (FFI), and Kuru (45). Prusiner et al. proposed the prion hypothesis that the agent causing TSE consists exclusively of a protein, termed prion (proteineous infectious particles) (Fig. 1) (44). The hypothesis states that interaction between an exogenously introduced abnormal isoform of prion protein (PrP^{Sc}) and the endogenous cellular isoform of prion protein (PrP^C), which is further converted into PrP^{Sc}, is essential (45). With the conversion, an accumulation of PrP^{Sc} and deficiency of PrP^C occurs, i.e. a

**Address correspondence to* Dr. Akikazu Sakudo, Department of Virology, Research Institute for Microbial Diseases, Osaka University, 3–1 Yamadaoka, Suita, Osaka 565–0871, Japan. Fax: +81–6–6879–8310. E-mail: sakudo@biken.osaka-u.ac.jp

Abbreviations: BSE, bovine spongiform encephalopathy; CJD, Creutzfeldt Jakob disease; CNS, central nervous system; CWD, chronic wasting disease; DAPI, 4′,6′-diamino-2-phenynlindole dihydrochloride; Dpl, Doppel; ELISA, enzyme-linked immunosorbent assay; ERK, extracellular signal-regulated kinase; ES, embryonic stem; FFI, fatal familial insomnia; FSE, feline spongiform encephalopathy; GSS, Gerstmann-Sträussler-Scheinker Syndrome; HR, hydrophobic region; LDH, lactate dehydrogenase; MAPK, mitogen-activated protein kinases; OR, octapeptide repeat region; PI, phosphatidylinositol; PKA, protein kinase A; *Prnp*, prion protein gene; PrP, prion protein; PrP^C, cellular isoform of prion protein; PrP^{Sc}, abnormal isoform of prion protein; SIN-1, 3-morpholinosydnonimine; SOD, superoxide dismutase; STAT, signal transducer and activator of transcription; STI1, stress-inducible protein 1; SV40 LTag, Simian Virus 40 Large T antigen; TME, transmissible mink encephalopathy; TSE, transmissible spongiform encephalopathy.

"gain-of-function" of PrP^{Sc} and "loss-of-function" of PrP^{C}, respectively, thought to be important etiological events in prion diseases (83). Therefore, it is important to characterize the functions of PrP^{C} and the mechanisms converting PrP^{C} to PrP^{Sc} in order to understand the infectious etiology of this disease. *In vivo* studies using prion protein (PrP)-knockout mice are usually performed to better understand PrP functions and the prion infection mechanism. PrP^{C}-deficient mice with brain homogenate from scrapie-infected mice are resistant to prion diseases (7) and do not show any replication of the agent (52). In contrast, some minor phenotypic defects in PrP-knockout mice have been observed, some of which may be related not to PrP function but to destruction of the splicing acceptor of the PrP gene (*Prnp*) in some $Prnp^{-/-}$ mouse lines (38, 58, 81). Furthermore, large numbers of animals are required for *in vivo* analyses of prion infection, while detailed *in vitro* analyses using culture systems are suitable for the study of PrP^{C} functions and prion infections, thus replacing the need for a large number of animals.

Primary cultured neurons have certain limitations, such as small culture size, short life span during cultivation, and the potential for contamination by other cells, whereas cell lines can be ultimately cultured providing large and pure populations of specific cell types. Therefore, if a detailed analysis is necessary, the use of cell lines is the most appropriate approach. PrP^{C} is highly expressed in neurons, and after a prion infection, PrP^{Sc} is accumulated in neurons, most of which can be cultured for only several weeks. Furthermore, the effective transfection of genes, which is required for a detailed functional analysis, is difficult especially in primary cultured neurons. Although PrP^{C} is highly expressed in most neurons and glia, PrP^{Sc} accumulates in specific regions of the brain depending on the strain of prion (20). Therefore, it is clear that a detailed analysis using many kinds of cells from many regions is needed to fully understand prion biology.

Cultured cell lines have made a great contribution to the recent progress involving research in basic and applied cell biology. For instance, several cell lines have been established for studying for prion infection mechanisms (3, 8, 11, 29, 47, 51, 68). These include several prion-susceptible cell lines such as neurohypothalamic GT1 cells and sub-lines of neuroblastoma N2a cells (4, 37, 63). Studies from *in vivo* and *in vitro* have shown that PrP^{C} is strictly required for prion infections, indicating that it would be a great advance if we could develop PrP-deficient cell lines for use in wider investigations in the field of prion biology. PrP-deficient cell lines have been established from PrP-deficient mice by several independent groups (58). Although these cell lines have been used mainly for studies on PrP func-

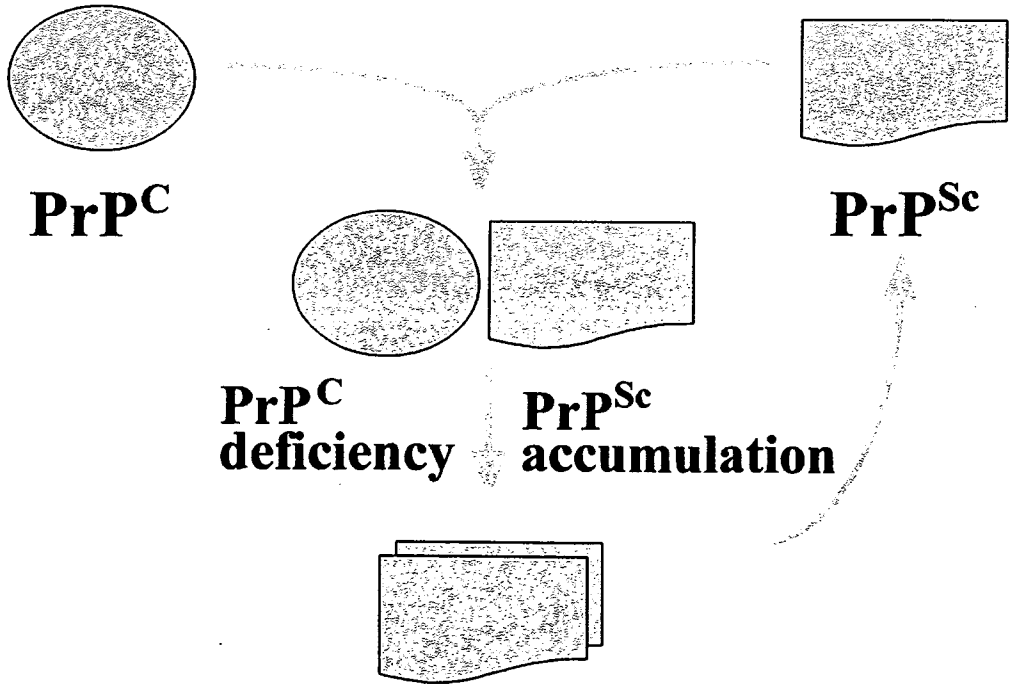

Fig. 1. Prion hypothesis. Interaction between an exogenously introduced abnormal isoform of prion protein (PrP^{Sc}) and the endogenous cellular isoform of prion protein (PrP^{C}), which is further converted into PrP^{Sc}, is essential for the prion hypothesis. With the conversion, PrP^{Sc} accumulation and PrP^{C} deficiency occur, i.e. a "gain-of-function" of PrP^{Sc} and "loss-of-function" of PrP^{C}, respectively, thought to be important etiological events in prion diseases.

tions so far, it should be noted that they also have several advantages over preexisting cell lines when it comes to studying prion infections.

In this review, we shall focus on recent findings about prion biology made possible by the availability of *Prnp*-deficient cell lines, which have improved our understanding of PrP functions, and also introduce potential contributions to the study of prion infection mechanisms.

Prnp-Deficient Cell Line for Studying the Functions of PrP^C

In recent years, efforts have been made to understand the functions of PrP^C. PrP-deficient cell lines have been used in some of these analyses. PrP-deficient cell lines include neuronal precursor cells, neuronal cells, skin fibroblasts and glial cells, whose characterization has been determined by the expression of marker proteins specific for cell types (58). Methods used for the production of cell lines have varied and include retrovirus-mediated method, lipofection of oncogenes, and fusion of primary cultured cells with carcinoma cells (58). These cell lines have been instrumental in elucidating several of the signal transduction pathways leading to anti-apoptotic and anti-oxidative functions (58). Especially, the neuroprotective function of PrP was strongly suggested by the PrP-deficient cell lines or other cell lines. For example, we have reported that PrP^C prevents cell death in $Prnp^{-/-}$ neuronal cell line HpL3-4 (28) (Fig. 2) and further found decreased expression of the anti-apoptotic proteins Bcl-2 and Bcl-xL in HpL3-4 cells during apoptosis induced by serum deprivation and suppression of the apoptosis on overexpression of Bcl-2 and Bcl-xL (55). Moreover, a greater increase in caspase-3/9 activation after serum deprivation was observed in HpL3-4 cells compared to HpL3-4 cells transfected with *Prnp* (56). These results suggest that the cell death in this model system is apoptotic, and the mitochondrial pathway plays an important role in the apoptosis of HpL3-4 cells (55, 56).

The general observation that an increase in reactive oxygen species induced by serum deprivation was observed before the onset of apoptosis (62) prompted our investigation into the importance of oxidative stress for PrP functions. From experiments using flow cytometry with a fluorescent dye reacting with superoxide anion and hydrogen peroxide, it was concluded that PrP activates cellular superoxide dismutase (SOD) activity and decreases superoxide anion and simultaneously shows transient increases of hydrogen peroxide (56). Therefore, the SOD activation suggests a contribution by PrP-expressing cells to resistance to serum deprivation.

Cellular prion protein PrP^C contains two evolutionarily conserved domains among mammals: namely, the octapeptide repeat region (OR; amino acid residue 51–90 in mouse PrP) and the hydrophobic region (HR; amino acid residue 112–145 in mouse PrP), while Doppel (Dpl) structurally resembles an N-terminally truncated PrP. Therefore, to further investigate the mechanisms by which PrP^C prevents apoptosis, the apoptosis of $Prnp^{-/-}$ cells and $Prnp^{-/-}$ cells expressing the wild-type PrP^C, PrP^C lacking OR and HR, or Dpl fused with OR and/or HR under serum-free conditions was examined (32, 54). The anti-apoptotic function of PrP deletion constructs, PrP-Dpl fusion constructs, and the control constructs were tested following stable transfection into *Prnp*-deficient neuronal HpL3-4 cells {HpL3-4 cells expressing wild-type PrP (HpL3-4-PrP), PrP(Δ53–94, Q52H) (HpL3-4-Δ#1), PrP(Δ95–132) (HpL3-4-Δ#2), PrP(Δ124–146) (HpL3-4-Δ#3), Dpl (HpL3-4-Dpl), Dpl fused with PrP(1–95) [HpL3-4-PrP(1–95)/Dpl], and Dpl fused with PrP(1–124) [HpL3-4-PrP(1–124)/Dpl] or the empty vector per se (HpL3-4-EM)}. In the absence of serum, HpL3-4, HpL3-4-EM, HpL3-4-Δ#1, HpL3-4-Δ#2, HpL3-4-Dpl, and HpL3-4-PrP(1–95)/Dpl cells undergo cell death with features of apoptosis, whereas HpL3-4-PrP, HpL3-4-Δ#3 and HpL3-4-PrP(1–124)/Dpl cells are resistant to serum deprivation (32, 54, 56). This tendency was revealed by a lactate dehydrogenase (LDH) assay, 4′,6-diamido-2-phenylindole hydrochloride (DAPI) staining, measurements of DNA content with flowcytometry, measurements of histone-associated DNA fragments (mono- and oligonucleosomes) in cytosolic fractions of the cells with an enzyme-linked immunosorbent assay (ELISA), and a DNA ladder assay. To further examine whether the susceptibility of each deletion mutant to serum deprivation was correlated with the activity of SOD, SOD activity in the presence and absence of serum was analyzed in each deletion mutant. The results supported our hypothesis that susceptibility to serum deprivation is correlated with SOD activity (Fig. 3). In fact, HpL3-4-Δ#1 cells demonstrated significantly lower levels of SOD activity than HpL3-4-EM cells, whereas HpL3-4-PrP and HpL3-4-Δ#3 cells showed significantly higher levels than HpL3-4-EM cells under serum deprivation for 6 hr. In contrast, HpL3-4-Δ#2 cells showed a level of SOD activity comparable with that of HpL3-4-EM cells. Taken together, the data presented here suggest that the anti-apoptotic function of PrP^C can be regulated by not only the OR but also the N-terminal half of HR, and this quantitative difference in the anti-apoptotic function of PrP deletion mutants correlates with the level of SOD activity in transfectants

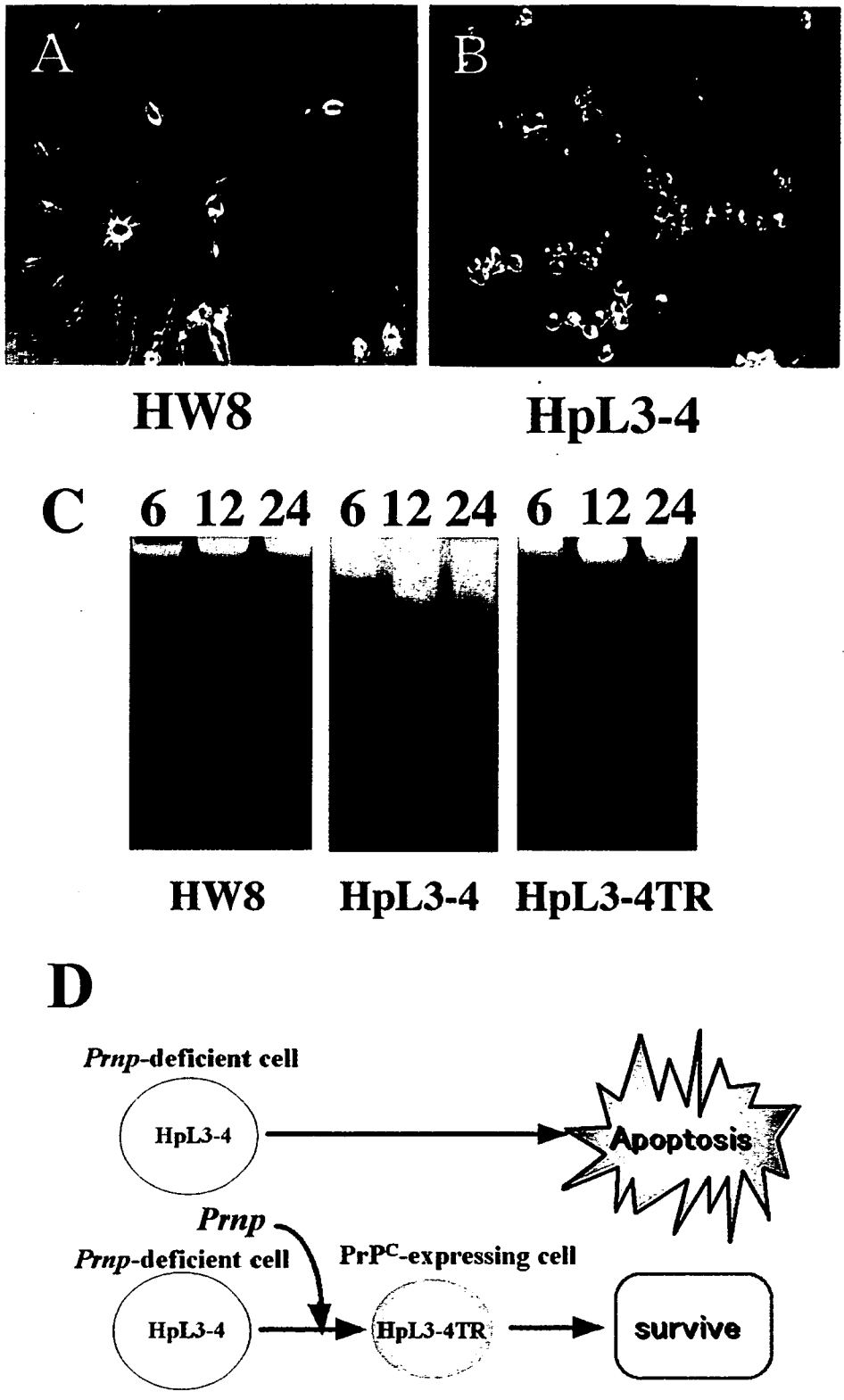

Fig. 2. Prion protein (PrP) prevents cell death in PrP gene (*Prnp*)-deficient neuronal cell lines. (A–B) The morphology of HW8 ($Prnp^{+/+}$) (A) and HpL3-4 ($Prnp^{-/-}$) (B) cells under serum deprivation was observed by phase-contrast microscopy. (C) HW8, HpL3-4, and HpL3-4TR ($Prnp^{-/-}$ cells transfected with the PrP-expression vector) cells serum-deprived for the indicated hours were analyzed by DNA ladder assay. HpL3-4 cells exhibited a longer DNA ladder than HpL3-4TR cells, suggesting that PrP expression prevents the induction of apoptosis of $Prnp^{-/-}$ cells. (D) Schematic presentation of the above results. After serum deprivation, HpL3-4 cells show apoptosis, whereas HpL3-4-TR cells are resistant to serum deprivation. These results suggest that PrP plays important roles in cell survival. Modified from Fig. 1 in Kuwahara et al. (28) and Fig. 3 in Onodera et al. (38) with permission from Nature Publishing Group and Center for Academic Publications Japan, respectively.

expressing the mutants (Fig. 3). The data are consistent with the notion that both the OR and N-terminal half of HR are necessary for activation of cellular SOD.

Next, we performed an investigation of whether stress-inducible protein1 (STI1) and copper are important for the biological activities displayed by PrP^C. The effect of the inhibitory peptides against PrP^C-STI1 binding and cellular copper concentrations in *Prnp*$^{-/-}$ cells was compared to that in PrP^C-expressing *Prnp*$^{-/-}$ cells under serum-free conditions (53, 57). STI1 and copper are reported to bind HR and OR (6, 33, 84), respectively, which are required for the anti-apoptotic and anti-oxidative functions of PrP in our experimental systems. The inhibitory peptides have a toxic effect on PrP^C-expressing cells by inhibiting the SOD activity, although this is not the case for *Prnp*$^{-/-}$ cells (53). Furthermore, immunoprecipitation indicated that STI1 interacted with the PrP^C in PrP^C-expressing cells (53). Moreover, the cellular copper concentration was decreased in *Prnp*$^{-/-}$ cells but not in PrP-expressing cells under oxidative conditions (57). Therefore, we concluded that PrP^C cooperates with STI1 and copper to activate SOD *via* OR and HR (Fig. 4). We also have reported that increased production of viruses such as coxsackievirus B3 and poliovirus in HpL3-4 cells suggests that PrP may be involved in the inhibition of viral replication as well as functions against virus-induced apoptosis (1, 36). In addition, we have recently established an NpL1 and NpL2 PrP-deficient cell line derived from ZrchI PrP-deficient mice (T. Nishimura, A Sakudo and T. Onodera, unpublished results). The truncated PrP (23–230 PrP) accumulated in the nucleus *via* interaction with chromatin and was not toxic to NpL1 cells (12). The truncated form of PrP corre-

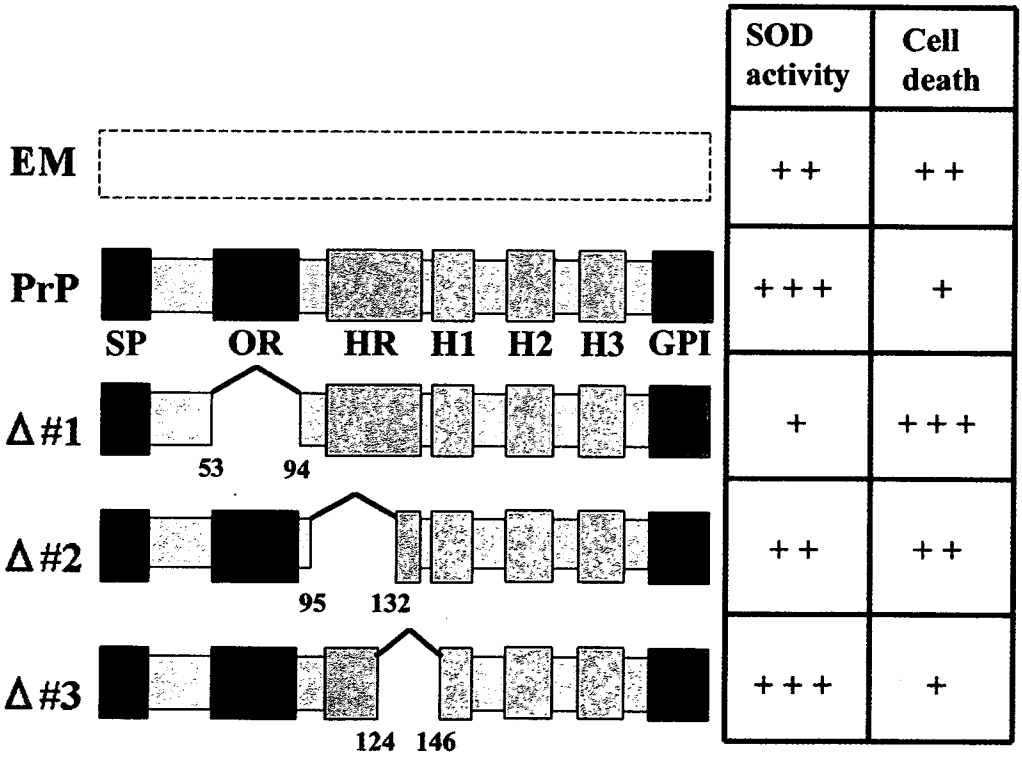

Fig. 3. Octapeptide region (OR) and N-terminal half of hydrophobic region (HR) are required for prion protein (PrP)-dependent superoxide dismutase (SOD) activation and anti-apoptotic function of PrP. Schematic representations of deletion mutants of mouse PrP are shown on the left. Locations of the deletions of mutants of mouse PrP [PrP: wild-type PrP; Δ#1: PrP(Δ53–94, Q52H); Δ#2: PrP(Δ95–132); Δ#3: PrP(Δ124–146)] as compared with the wild-type protein are shown by a space within the bar next to the indicated protein. Numbers refer to the amino acid residues in the mouse PrP sequence. The OR, HR, signal peptide sequence (SP) and α-helix 1–3 (H1–H3) are shown. PrP has a glycosylphosphatidylinositol (GPI) anchor attached to its C terminus. HpL3-4 cells expressing PrP, Δ#1, Δ#2 and Δ#3 or the empty vector per se (EM) were serum deprived for 24 hr, when maximum apoptosis occurs, and the SOD activity of the cells after serum deprivation for 6 hr, when reactive oxygen species start to be generated, is shown on the right. The number of pluses (+) indicates the degree of apoptosis or SOD activity. Modified from Fig. 4 in Sakudo et al. (58) and Fig. 1 in Sakudo et al. (54) with permission from Bentham Science Publishers, Ltd. and Elsevier, Ltd., respectively.

sponding to amino acid residues 23–230 had anti-oxidative activity similar to wild-type PrP and showed nuclear localization in N2a and NpL1 cells.

Other groups have also studied PrP functions using HpL3-4 cells and other cells. A Korean group confirmed our results and further found greater alteration of calcium ion, transmembrane potential and cytochrome c levels in mitochondria of HpL3-4 cells than those of HW8 cells after serum deprivation (25). They also recently independently established neuronal cell lines from hippocampal neurons of ZrchI PrP-deficient mice by lipofection of Simian Virus 40 Large T antigen (SV40 LTag)-expressing vector and found greater proliferation in neuronal cell lines from PrP-deficient mice (Zpl) than those of wild-type mice (ZW) (24). A French group also confirmed an increase in cell viability on the reintroduction of *Prnp* in HpL3-4 cells under serum deprivation (34). An Italian group investigated the signal cascade of apoptosis induced by serum deprivation and 3-morpholinosydnonimine (SIN-1), and showed that recruitment of phosphatidylinositol (PI) 3-kinase by PrP^C contributes to cellular survival toward oxidative stress by SIN-1 and serum deprivation in HpL3-4 cells (74). A Japanese group established SFK-B and SFK-C skin fibroblast cell lines derived from continuous cultures of abdominal skin explants of Ngsk PrP-deficient mice. The SFK-B and SFK-C cells demonstrated decreased expression of Ras- and Rac-related proteins compared to wild-type skin fibroblast cell lines (60, 61). A British group established the neuronal cell line F14 by the fusion of PrP-knockout cerebellar cells and mouse neuroblastoma cells. The effect of PrP mutations on PrP membrane orientation was investigated using the F14 cells (21). They further have reported that the OR of PrP decreases copper toxicity independent of oxidative stress (18).

In summary, the STI1 and copper signaling pathways to SOD activation involved in the anti-apoptotic and

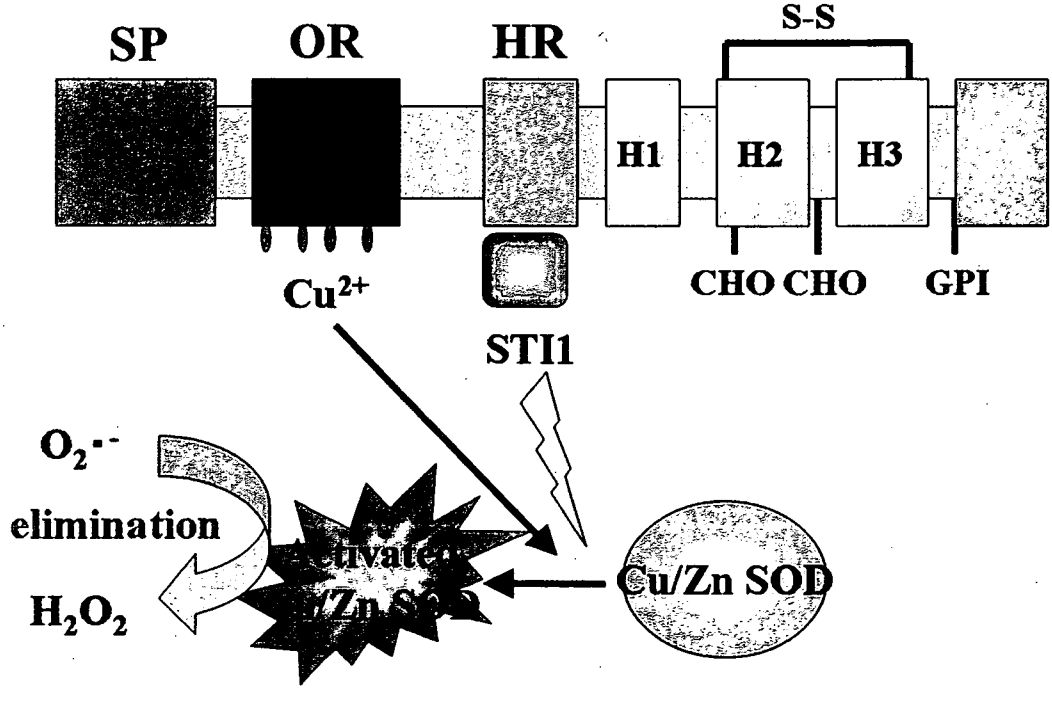

Fig. 4. Model of prion protein (PrP)-dependent superoxide dismutase (SOD) activation. After stress-inducible protein 1 (STI1) binds to the hydrophobic region (HR) in the cellular isoform of prion protein (PrP^C), STI1 may be activated by the octapeptide repeat region (OR), because both the OR and HR are indispensable for maximal-activation of cellular SOD. PrP^C is localized to the membrane, and STI1, to the membrane and cytosol (53, 84). Therefore, STI1 may be activated by PrP^C in the membrane. The activated STI1 may shift to the cytosol and activate Cu/Zn SOD. The hypothesis is consistent with the report that inhibition of binding between PrP^C and STI1 by inhibitory peptides decreases cellular SOD activity (53). The mechanisms of activation of STI1 by PrP^C or those of Cu/Zn SOD by STI1 remain unknown. Copper might play an important role in the mechanisms of PrP^C-dependent activation of Cu/Zn SOD because: (i) Deletion of OR decreases PrP^C-dependent activation of SOD, (ii) Activity of Cu/Zn SOD is regulated by copper incorporation (82), and (iii) Copper enhances endocytosis of PrP^C (41). The OR, HR, disulfides (S-S), two Asn-linked glycosylation sites (CHO), signal peptide sequence (SP) and α-helix 1–3 (H1–H3) are shown. PrP has a glycosylphosphatidylinositol (GPI) anchor attached to its C terminus.

anti-oxidative functions of PrP *via* OR and HR have been uncovered using PrP-deficient cells. These cells also provide information on the signaling cascade for the PrP-dependent pathway and important regions for the cellular distribution of PrP. Many questions, however, remain. To what extent the concentration of copper is involved in STI1-PrP^C or PrP^C signaling and what the other cellular effectors are still need to be elucidated. STI1 has to be present in both the cell membrane and cytosol, because PrP^C is localized mainly to the cell membrane, and Cu/Zn SOD to the cytosol. However, taking into consideration our results, potential cooperation between PrP, STI1, copper and Cu/Zn SOD is conceivable. Therefore, the role of the OR and N-terminal half of HR in the cooperation needs further study. Also, the contribution of other pathways such as cAMP/protein kinase A (PKA) (10, 33) and mitogen-activated protein kinases (MAPK) (33), the Fyn Src family of tyrosine kinases (35, 59), the extracellular signal-regulated kinase (ERK) pathway (10, 27, 39, 64), the anti-apoptotic phosphatidylinositol 3-kinase/Akt pathway (29, 69, 80), and signal transducer and activator of transcription (STAT)-1 (69) discovered using other experimental systems should be reconfirmed with experiments using PrP-deficient cell lines. In this regard, PrP-deficient cells can play a useful role. Ultimately though, it has to be confirmed which of these pathways regulates PrP-dependent anti-apoptotic and anti-oxidative functions. Finally, findings on the neuroprotective functions of PrP revealed using HpL3-4 cells, which are immortalized by SV40 LTag (28), will also stimulate interest to determine whether intercrosses of the "SV40 LTag transgenic mouse" (17) and *Prnp*$^{-/-}$ mouse result in modulated oncogenesis.

Potential of *Prnp*-Deficient Cells for Studying Prion Infections

A PrP-deficient cell line is useful not only for studying PrP functions but also for the analysis of prion infection.

Transgenic technology in mice is usually used to analyze specific amino acid residues and domains of PrP^C for prion infections and PrP^{Sc} accumulation (2, 9, 14, 15, 42, 66, 67, 73). From these studies, the incidence of natural sheep scrapie is associated with polymorphisms of the PrP gene, at codons 136, 154, and 171 (13). Furthermore, PrP-knockout mice overexpressing mouse PrP with a deletion or modification of OR show a decrease of prion infectivity (15, 67, 70, 71).

Although the results obtained from these experiments provide important information on prion biology, the production of transgenic mice is time-consuming and expensive, and thus not suited to a detailed analysis of PrP domains and amino acid residues using many kinds of PrP mutants. Additionally, the etiology induced by prion infections *in vivo* remains unclear: a cell-autonomous event in an independent cell or, rather, a systemic process involving a heterogeneous cell population in the brain. Cell culture models for prion infection will greatly help us to understand the molecular mechanisms of PrP^{Sc} formation and the role of the amino acid sequence and the structural domains of PrP in the conversion of PrP^C to PrP^{Sc} (22, 23, 76). So far, such experiments have employed persistently infected cell cultures such as ScN2a, ScHB and SMB (43, 50, 77). *De novo* infections of cell cultures with prions are restricted by relatively low infection efficiencies (46). Cell lines sometimes become susceptible to prions when co-expressed with endogenous PrP during infection experiments (46, 69, 75, 79). However, interference of endogenous PrP with the pathogenicity of TSE agents from other species has been reported (48, 49, 65, 72). Moreover, concomitant expression of heterogenous species of PrP seems to inhibit prion infections (Fig. 5), even if cell lines expressing undetectable levels such as rabbit kidney epithelial RK13 cells are used (75). Hence, the transfection of various deletion mutants into *Prnp*$^{-/-}$ cell lines lacking endogenous PrP will help us to analyze the real domain of PrP^C required for prion pathogenicity without interference with the endogenous PrP if followed with prion infection (Fig. 5). Therefore, we recently have focused on prion infection experiments using HpL3-4 cells expressing mouse PrP or hamster PrP (Sakudo, Wu, Onodera, Ikuta, unpublished results). After incubation with brain homogenates of chandler prion-infected mice or cell lysate of chandler prion-persistently infected ScN2a cells for 1 or 2 days, the cell cultures were passaged for 2 weeks, then PrP^{Sc} detection was performed by Western blotting with anti-PrP antibody SAF83. After chandler prion infection, the amount of PrP^{Sc} transiently increased in HpL3-4 cells expressing mouse PrP or hamster PrP for the first several passages then gradually decreased. PrP^{Sc} finally was undetectable by 2 weeks later. Further, our preliminary observations have found that HpL3-4-PrP and HpL3-4-Δ#2 showed a transient increase in the amount of PrP^{Sc} after infection of chandler prion from brain homogenates of infected mice or cell lysate of ScN2a, whereas HpL3-4-Δ#1 did not. These results are consistent with *in vivo* results using transgenic mice expressing mouse PrP with a deletion of OR (67) or hamster PrP chimera in OR (70, 71), and *de novo* generation of protease-resistant PrP from OR-deficient PrP in cell-free experiments (30, 31) showing